Predictability of atmospheric flow regimes on seasonal and sub-seasonal scales

Franco Molteni

ECMWF, Reading, U.K.

ECMWF

Outline

- Introduction:
  - Dynamical concepts
  - Overview of "essential" literature

- Detection of regimes in atmospheric and model datasets
  - PDF estimation in one or two dimensions
  - An example of cluster analysis for the North Atlantic domain

- Sources of extended-range predictability
  - Impact of external/boundary forcing on atmospheric regimes
  - Linear and non-linear impact of ENSO on regime properties
  - MJO and Euro-Atlantic regimes

Multiple equilibria, flow regimes and related dynamical concepts

Multiple equilibria:

Multiple stationary solutions of a non-linear dynamical system

Flow regime:

A persistent and/or recurrent large-scale flow pattern in a (geophysical) fluid-dynamical system

Weather regime:

A persistent and/or recurrent large-scale atmospheric circulation pattern which is associated with specific weather conditions on a regional scale

Flow regimes in non-linear systems

3-variable model of Rayleigh-Benard convection ***(Lorenz 1963)***

- $dX/dt = \sigma\,(Y - X)$
- $dY/dt = -\,X\,Z + \mathbf{r}\,X - Y$
- $dZ/dt = X\,Y - b\,Z$

Unstable stationary states

- $X = Y = Z = 0$
- $X = Y = \pm\,[\,b\,(\mathbf{r} - 1)]^{1/2}\;,\; Z = \mathbf{r} - 1$

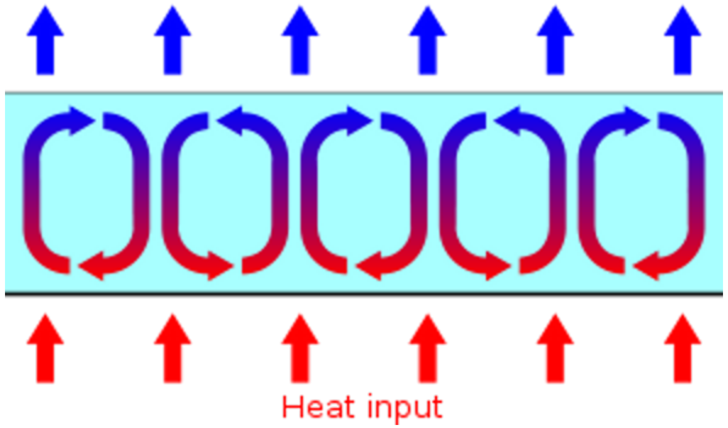

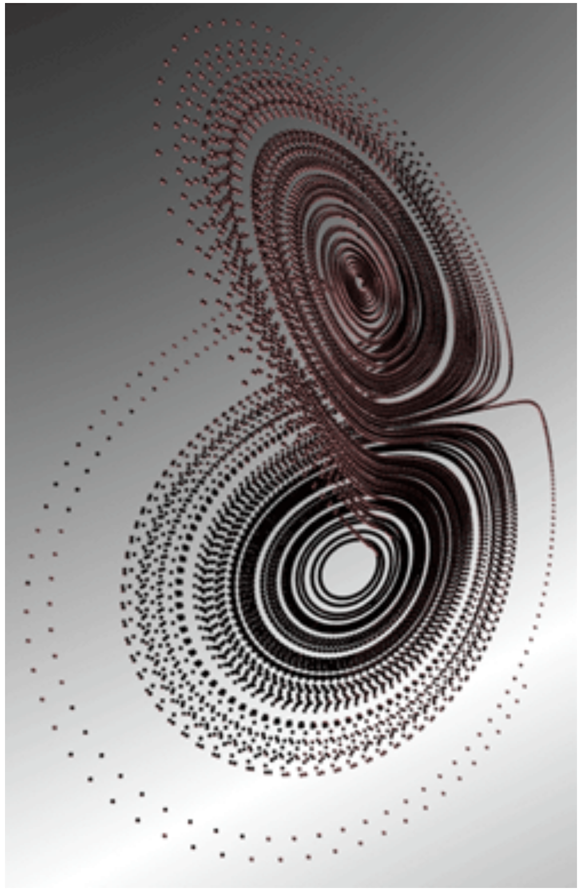

Atmospheric regimes as quasi-stationary states

q : barotropic or quasi-geostrophic potential vorticity

$$\partial_t q = - V_\psi \cdot \textit{grad}\ q - D\,(q - q^*)$$

steady state for instantaneous flow:

$$0 = - V_\psi \cdot \textit{grad}\ q - D\,(q - q^*)$$

steady state for time-averaged flow:

$$0 = - \langle V_\psi \rangle \cdot \textit{grad}\ \langle q \rangle - D\,(\langle q \rangle - q^*) - \langle V'_\psi \cdot \textit{grad}\ q' \rangle$$

Multiple equilibria: Charney and DeVore 1979

Multiple steady states of low-order barotropic model with wave-shaped bottom topography

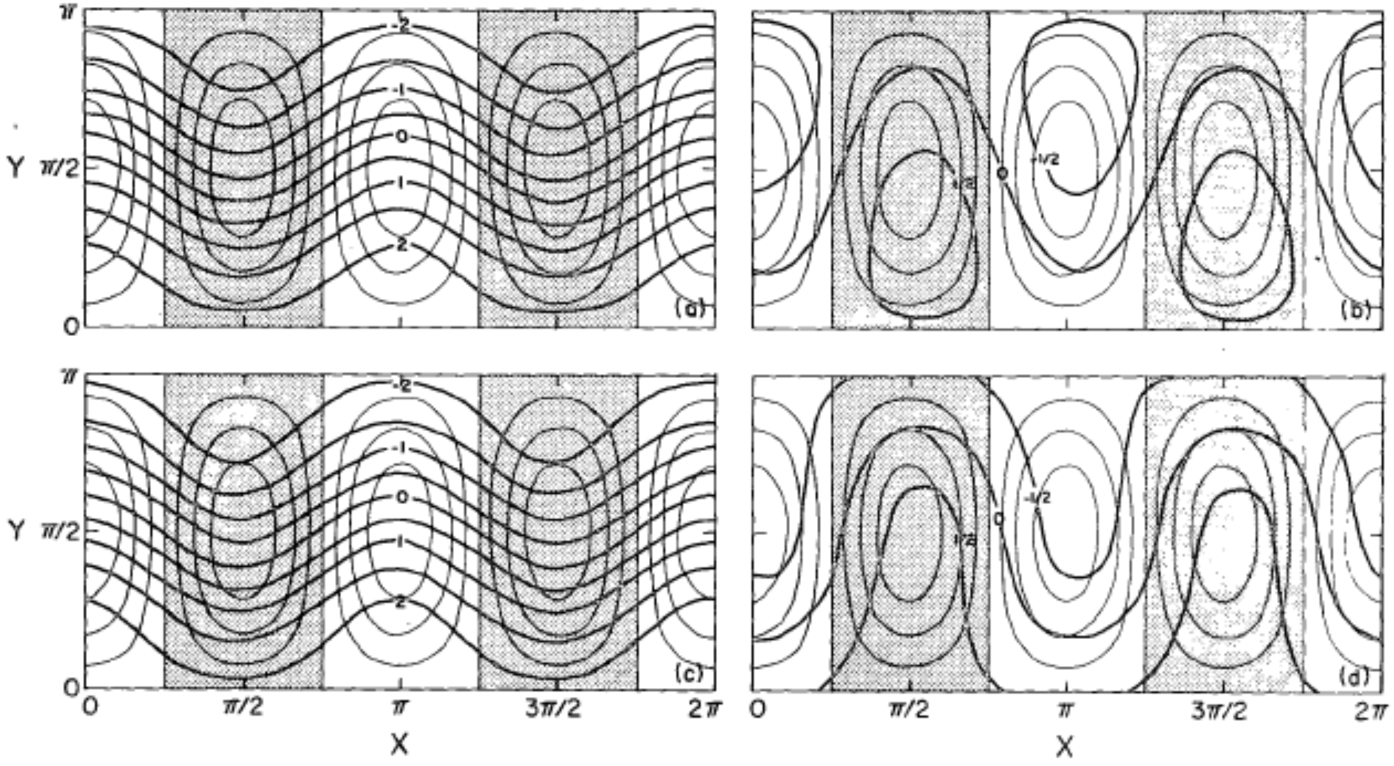

FIG. 4. Streamfunction fields of the stable first mode equilibria of a topographically forced flow for $k = 10^{-2}$, $L/a = ¼$, $n = 2$, $h_0/H = 0.2$ and $\psi_A^* = 0.2$: for the spectral model above resonance (a) and slightly below resonance (b); and for the grid-point model above resonance (c) and slightly below resonance (d). The nondimensional topographic heights are shown with light lines; the contour spacing is 0.05 units, with negative regions shaded.

Weather regimes: Reinhold and Pierrehumbert 1982

Hemispheric weather regimes arising from equilibration of large-scale dynamical tendencies and "forcing" from transient baroclinic eddies

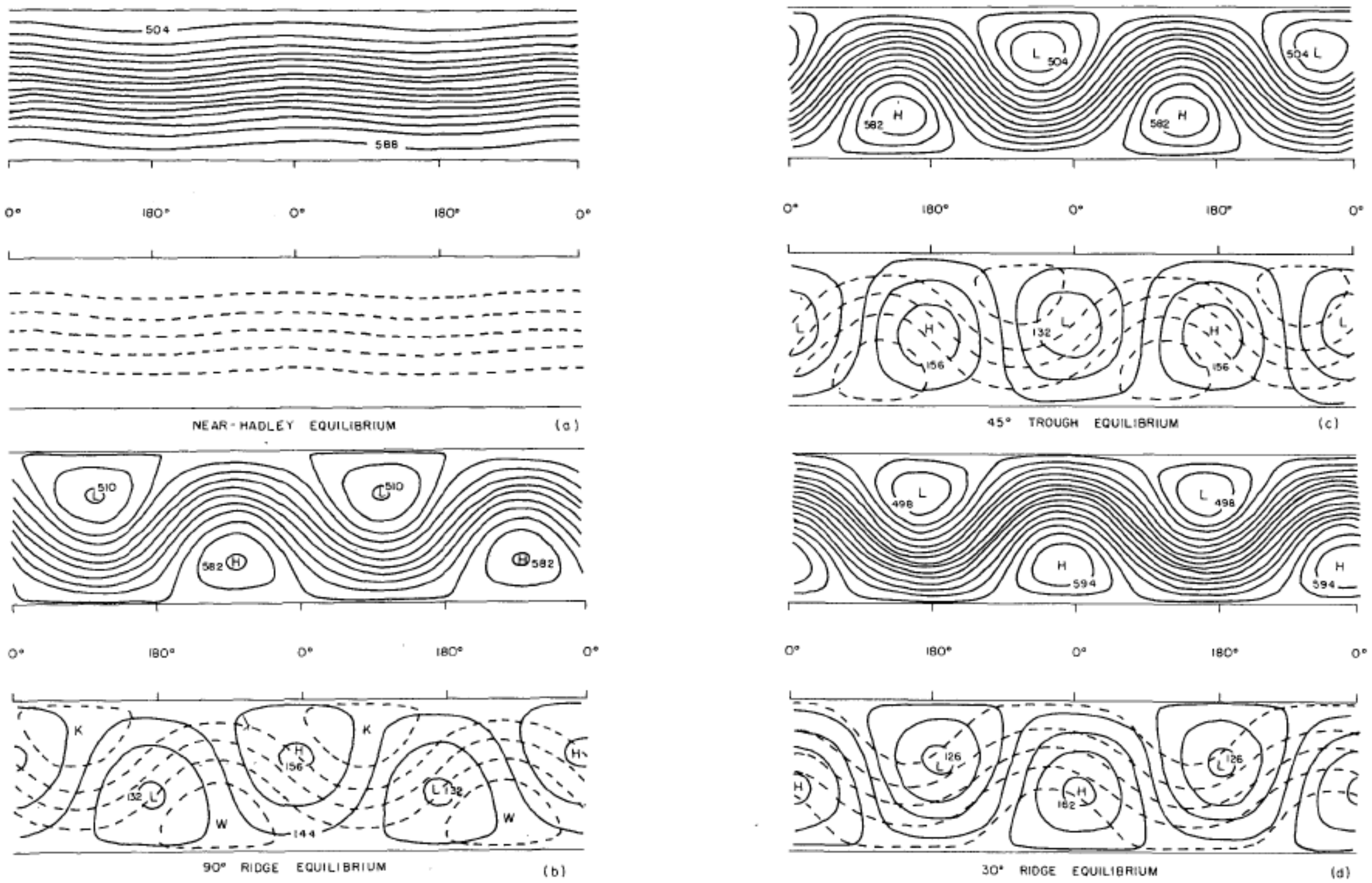

Eddy "forcing" of blocking regimes: the Imperial College school

- **Green 1977**: *The weather during July 1976: some dynamical consideration of the drought*

- **Illari and Marshall 1983**: *On the interpretation of eddy fluxes during a blocking episode*

- **Shutts 1986**: *A case study of eddy forcing during an Atlantic blocking episode*

- **Haines and Marshall 1987:** *Eddy-forced coherent structures as a prototype of atmospheric blocking*

Regional regimes: Vautard and Legras 1988

Regional weather regimes arising from equilibration of large-scale dynamical tendencies and PV fluxes from transient baroclinic eddies

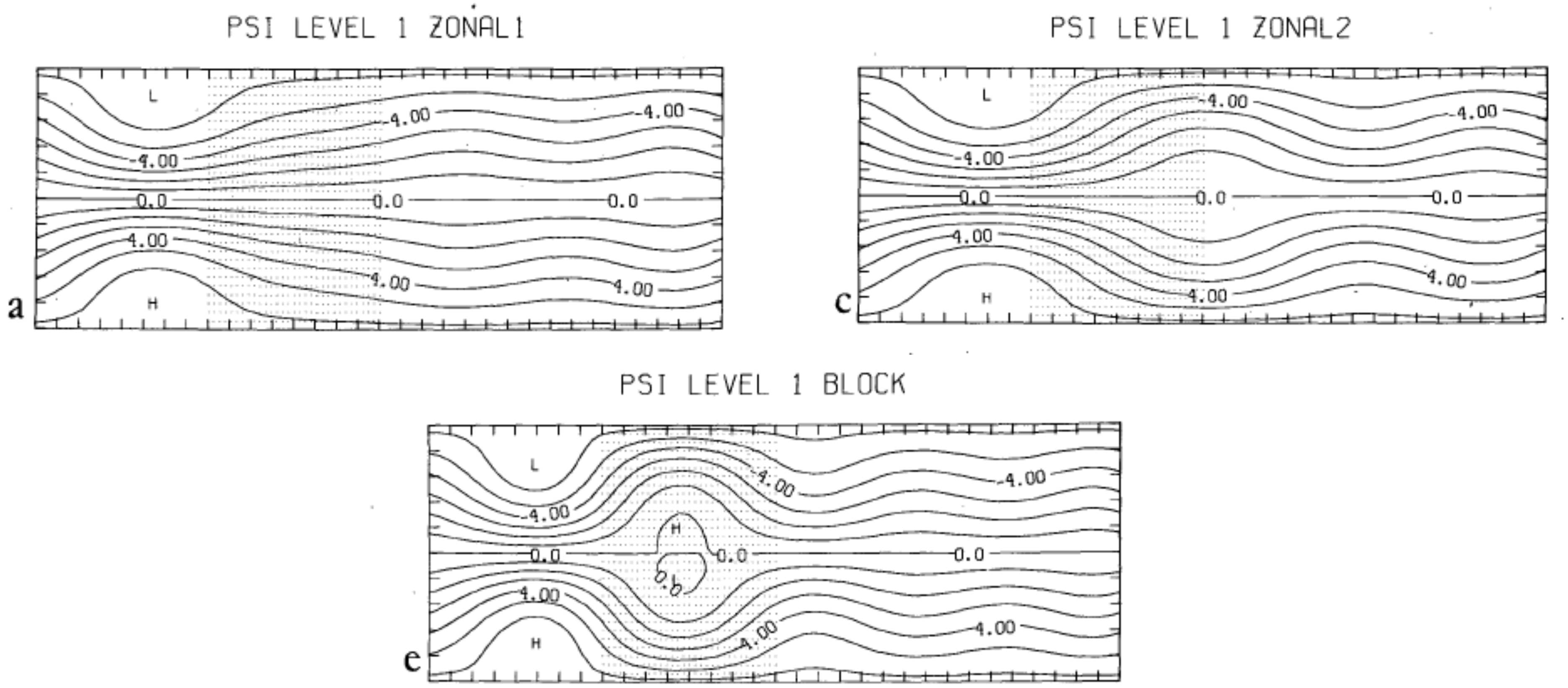

Bimodality in one-dim. PDF (Hansen and Sutera 1986)

Bimodality in the probability density function (PDF)
of an index of N. Hem. planetary wave amplitude
due to near-resonant wave-numbers (m=2-4)

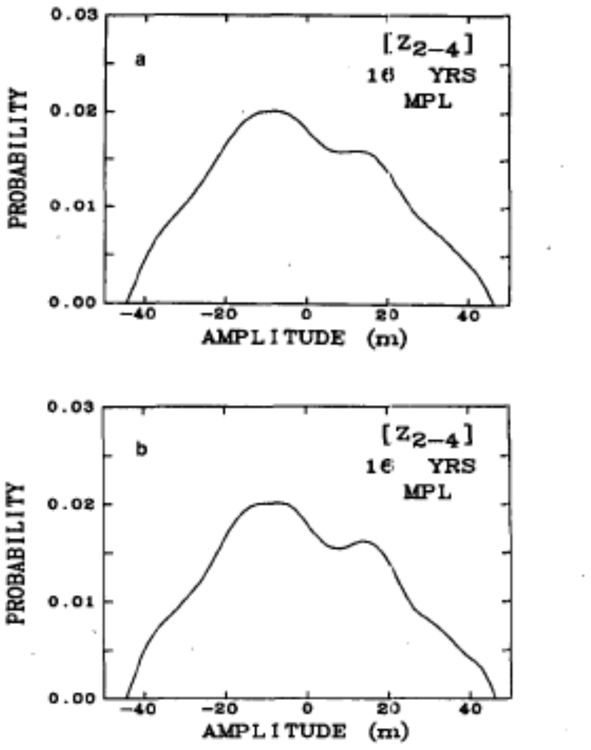

FIG. 4. MPL probability density estimates of $[Z_{2-4}]$ formed from the 16 winter composite filtered data for (a) $\alpha = 10^7$ and (b) $\alpha = 5 \times 10^6$.

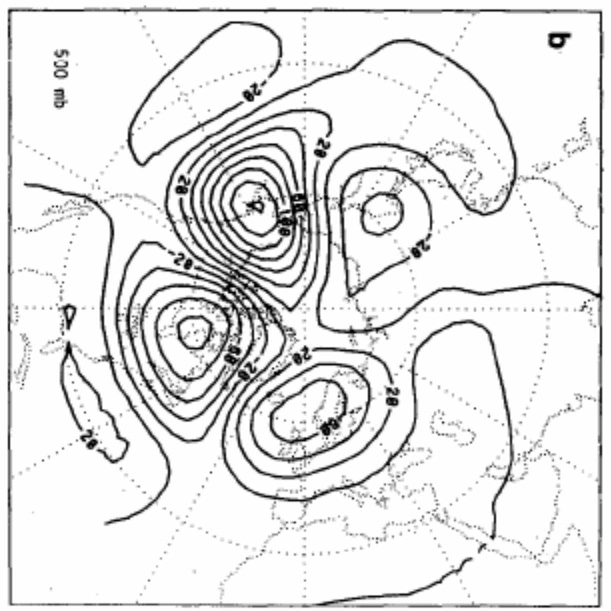

Regimes from 2-dim. PDF estimation (Corti et al. 1999)

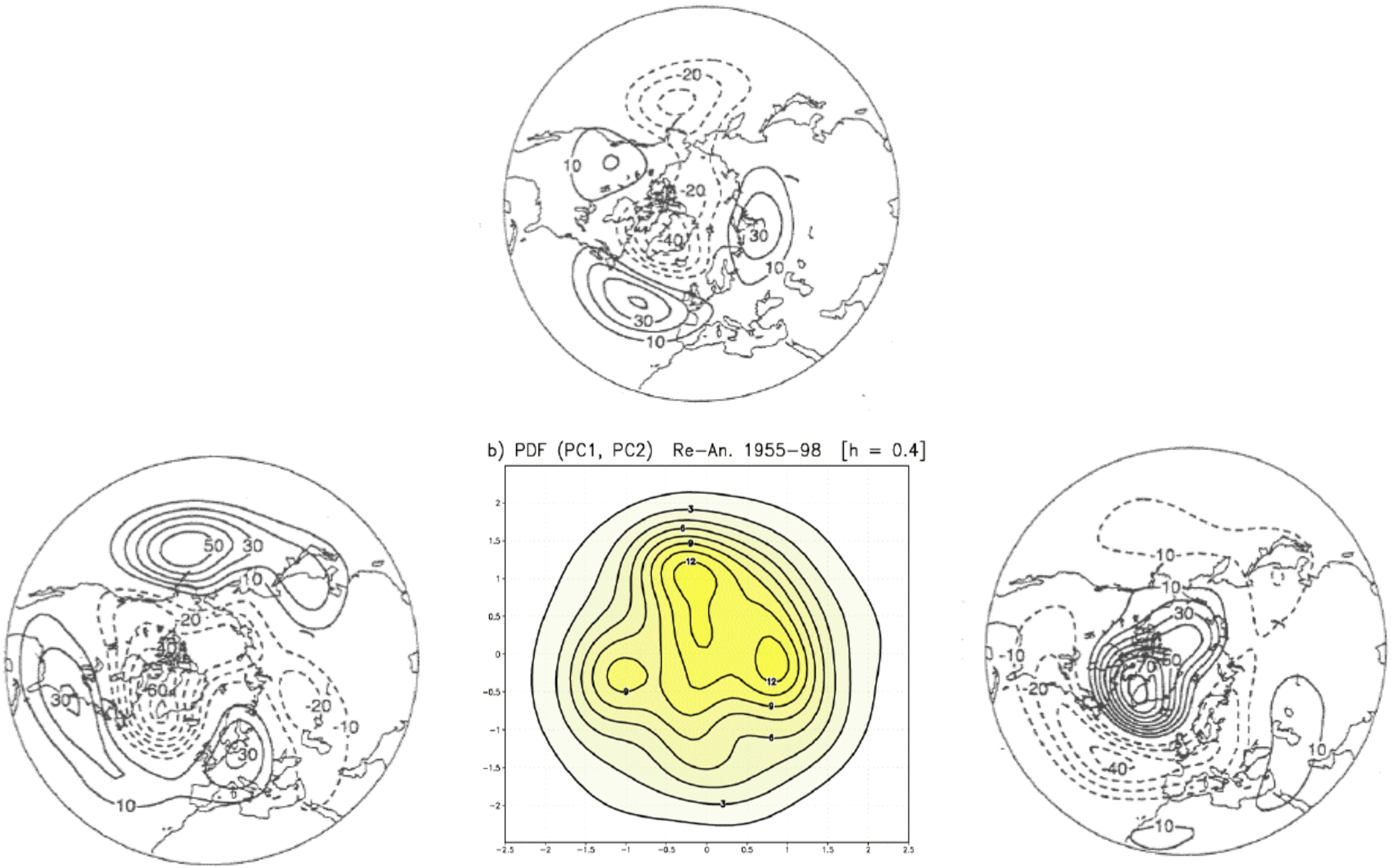

Regimes from cluster analysis (Michelangeli et al. 1995)

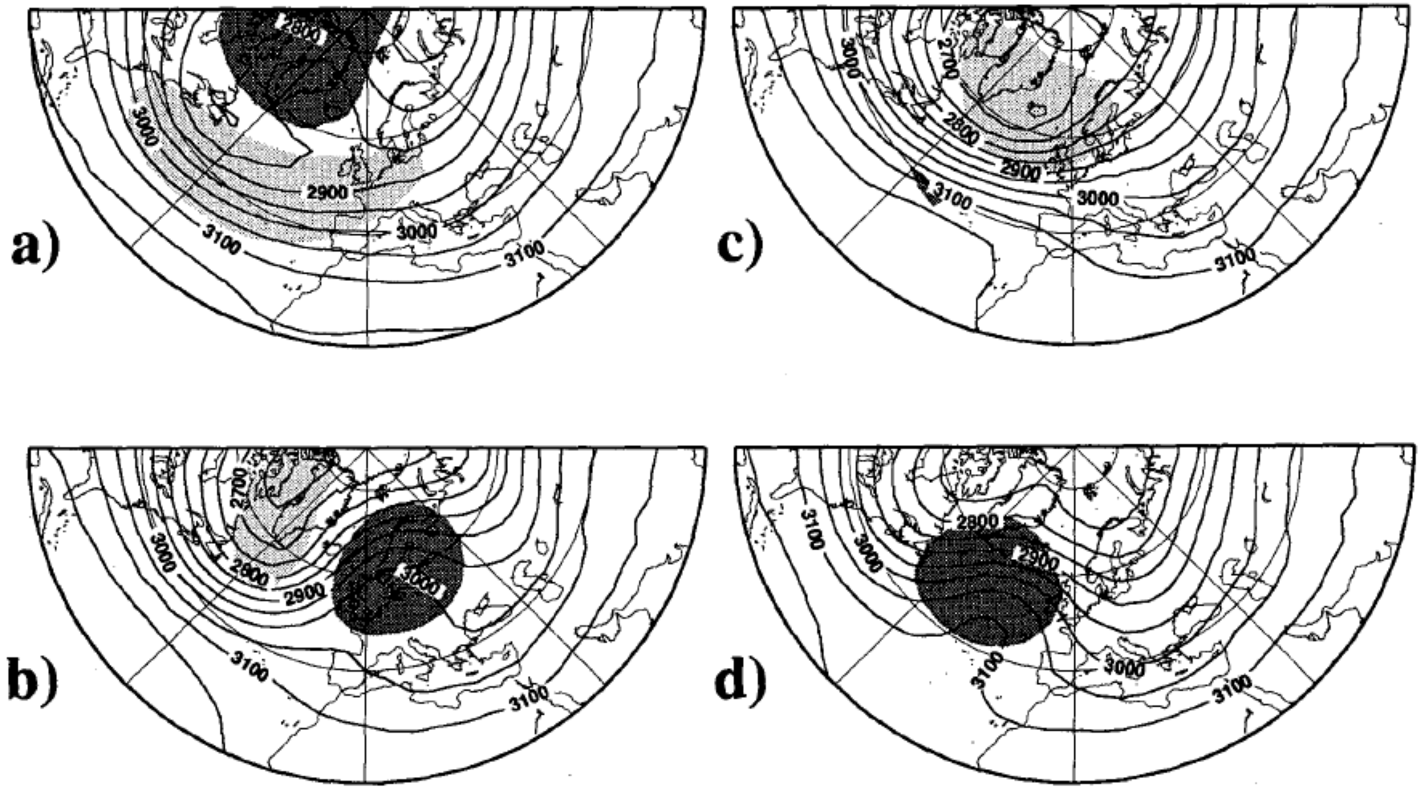

FIG. 4. Composites of the 700-hPa geopotential heights for the four clusters found over the ATL sector. Contour interval is 50 m. Dark shaded areas show areas where the anomaly of the composite with respect to the wintertime average is larger than 50 m. Light shaded areas correspond to anomalies lower than −50 m. Clusters are sorted by their consistency: (a) cluster 1; (b) cluster 2; (c) cluster 3; (d) cluster 4.

Regime behaviour and anomalous forcing

Lorenz (1963) truncated convection model with additional forcing (Molteni et al. 1993; Palmer 1993)

- $dX/dt = \sigma (Y - X)$
- $dY/dt = - X Z + r X - (Y - Y^*)$
- $dZ/dt = X Y - b Z$

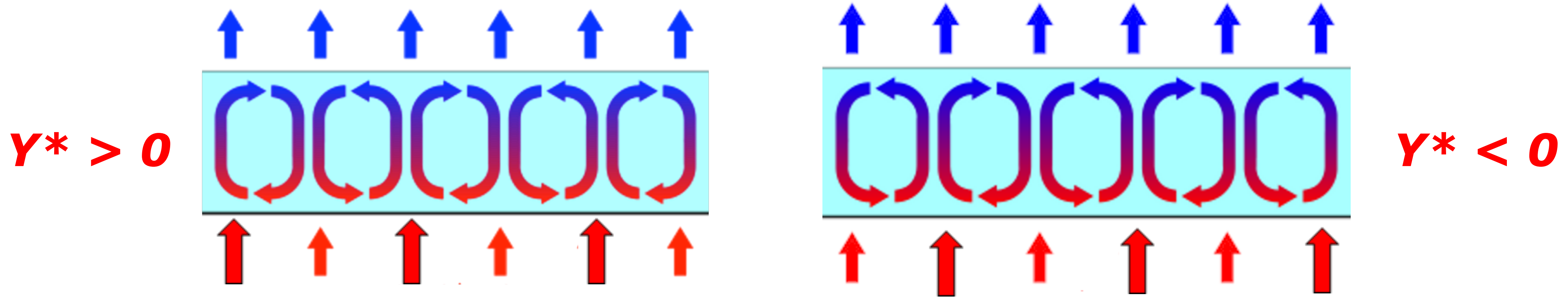

Impact of "external" forcing in non-linear systems

The properties of flow regimes may be affected by anomalous forcing in two different ways:

- **Weak forcing anomaly**: the number and spatial patterns of regimes remain the same, but their frequency of occurrence is changed
- **Strong forcing anomaly**: the number and patterns of regimes are modified as the atmospheric system goes through bifurcation points

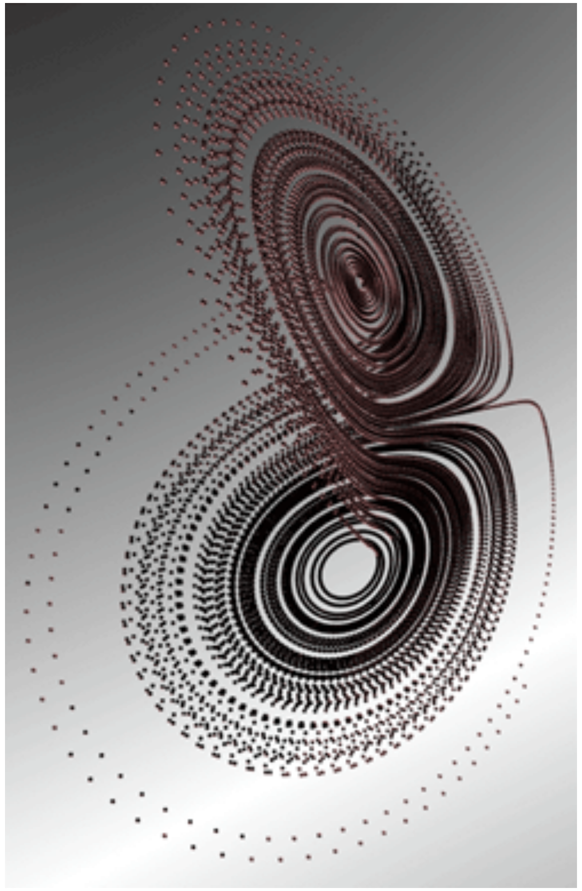

El Niño and the Southern Oscillation

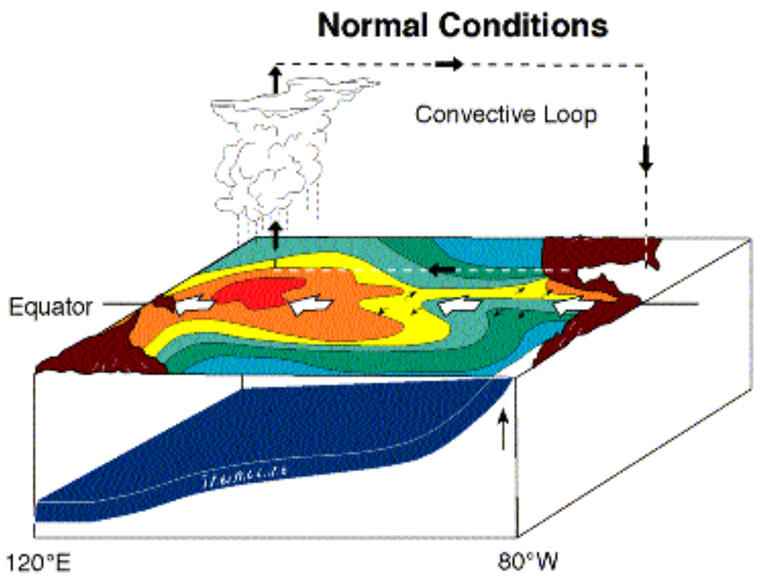

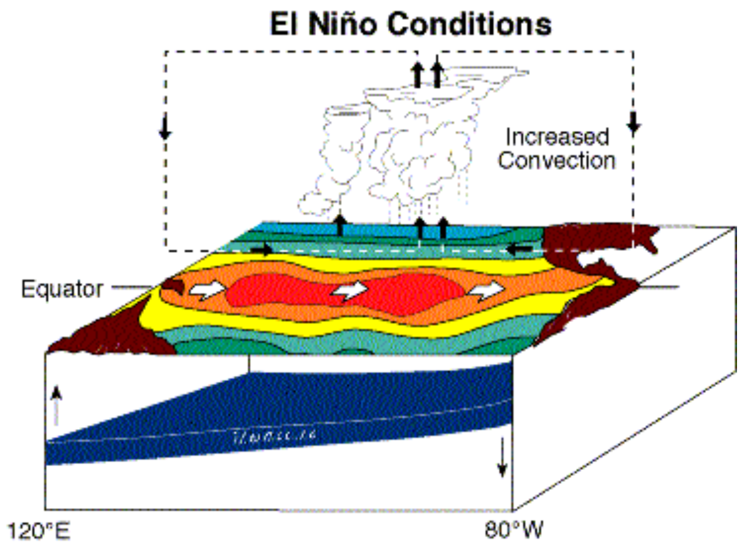

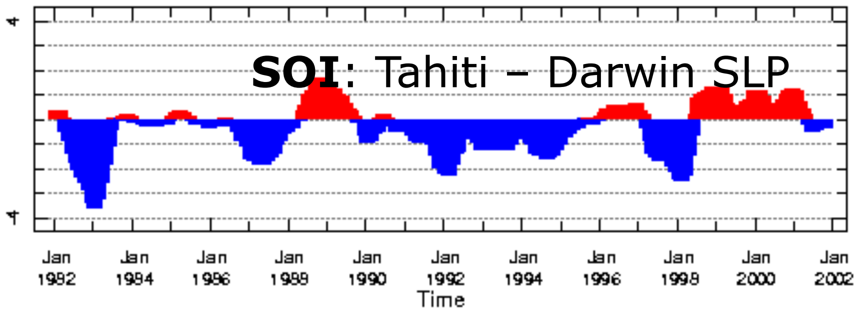

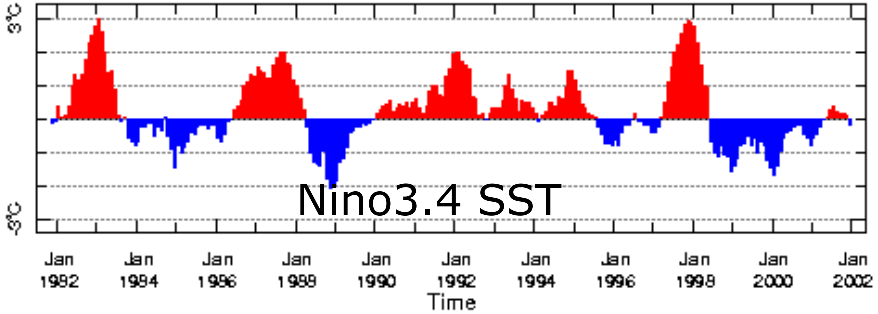

Extratropical teleconnections with ENSO

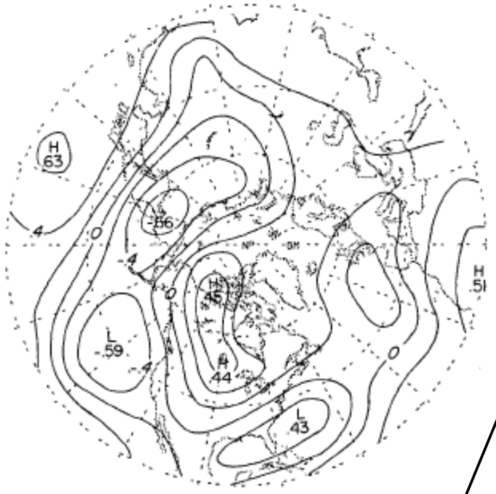

a

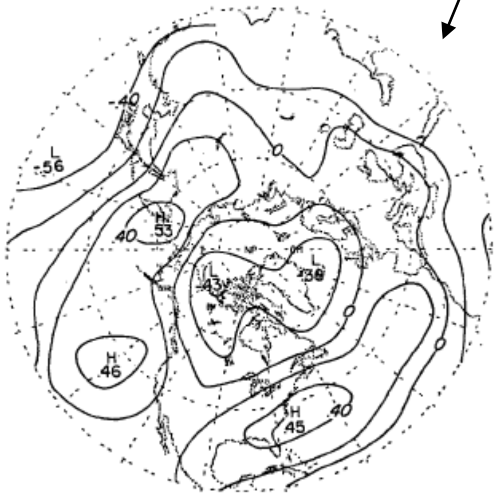

c

Correlation of 700hPa height with
a) PC1 of Eq. Pacific SST
c) SOI index

Schematic diagram of tropical-extratropical
teleconnections during El Niño

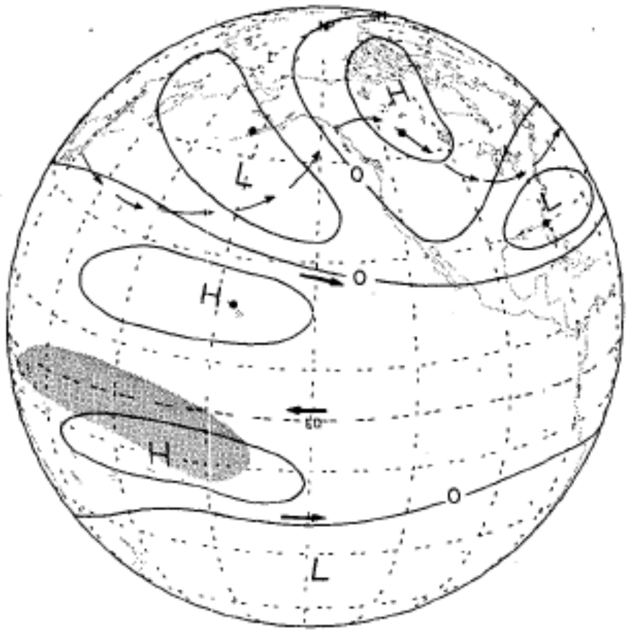

Horel and
Wallace 1981

A regime approach to seasonal predictions

Cluster analysis of low-frequency anomalies of Z 200 in NCEP re-analysis and COLA AGCM ensembles (Straus, Corti & Molteni 2007)

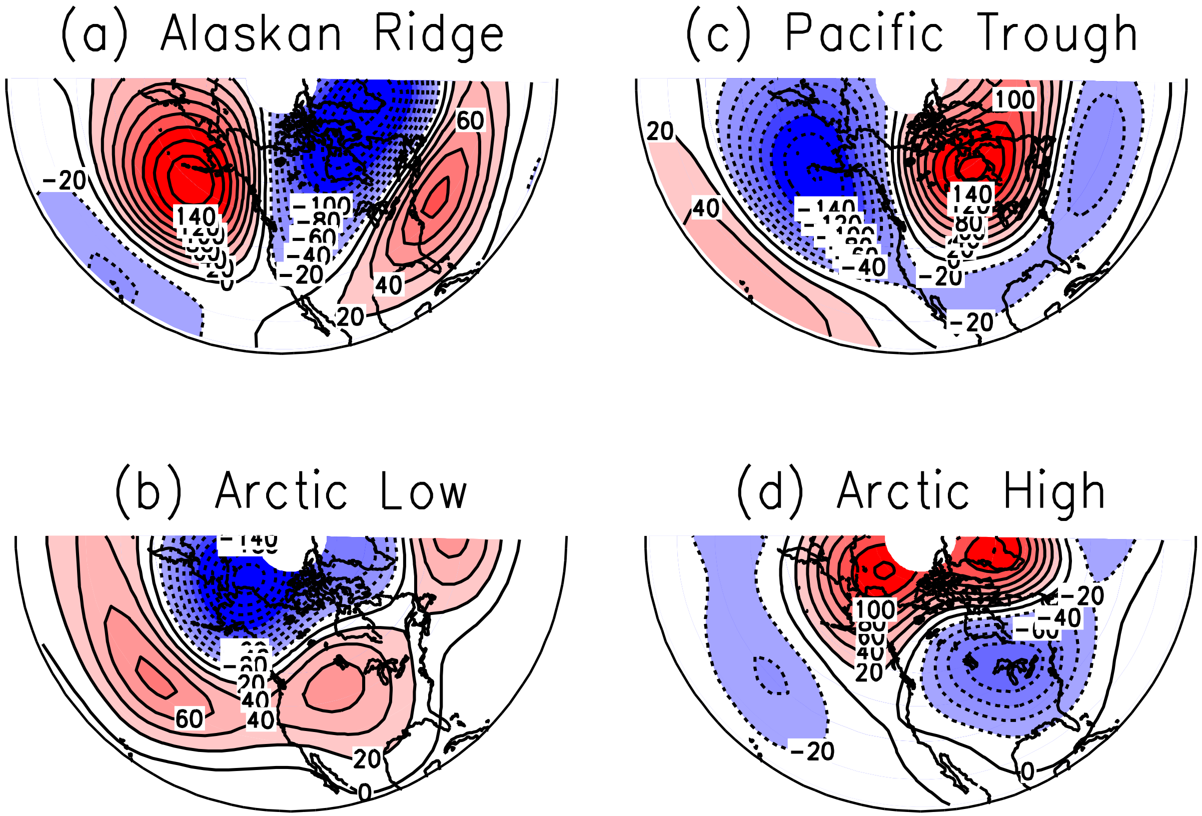

A regime approach to seasonal predictions

Predictability of cluster frequencies (SCM 2007)

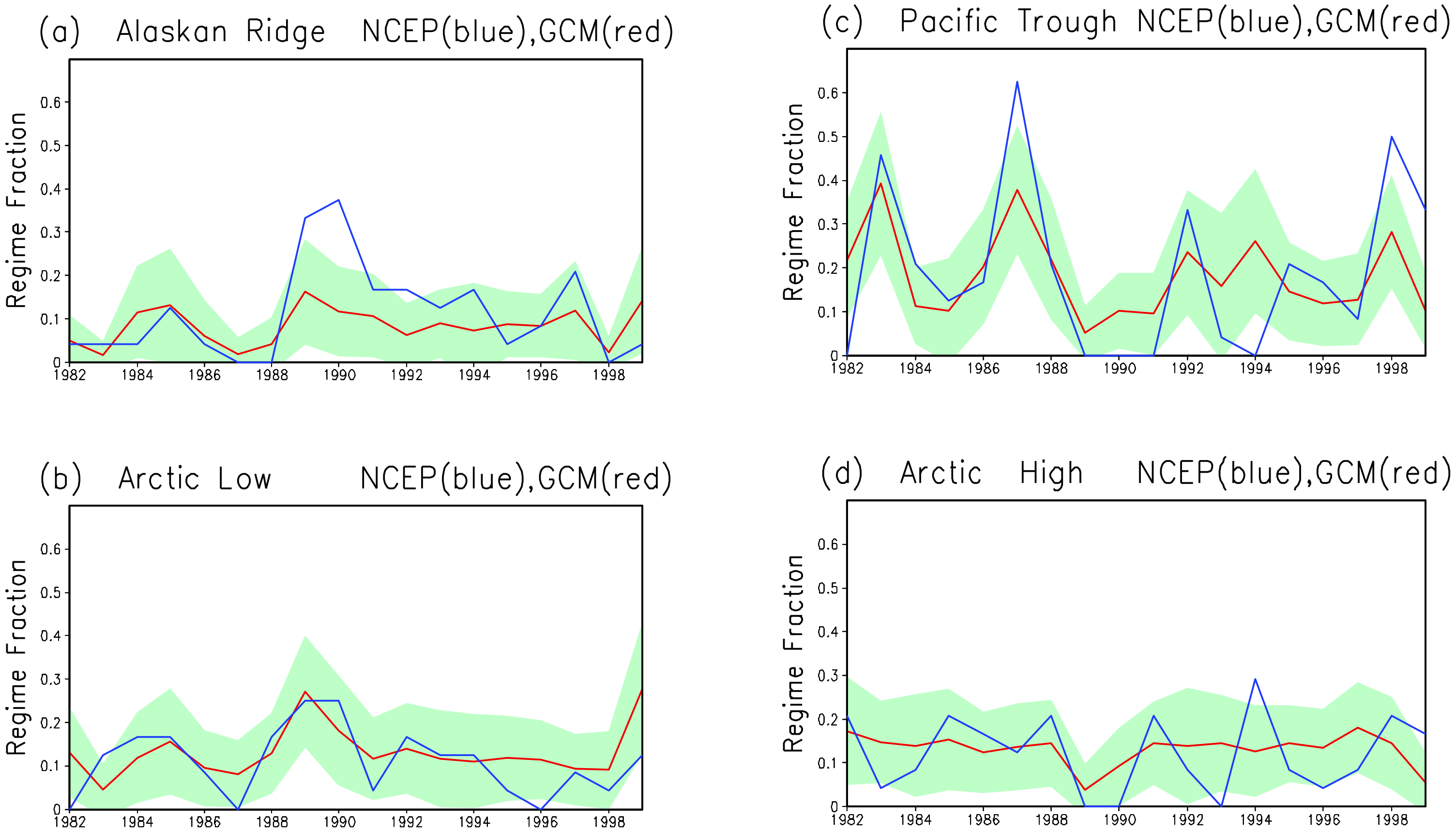

Does ENSO affect the number of regimes?

- Ratio of inter-cluster to intra-cluster variance as a function of ENSO indices (Straus and Molteni 2004)

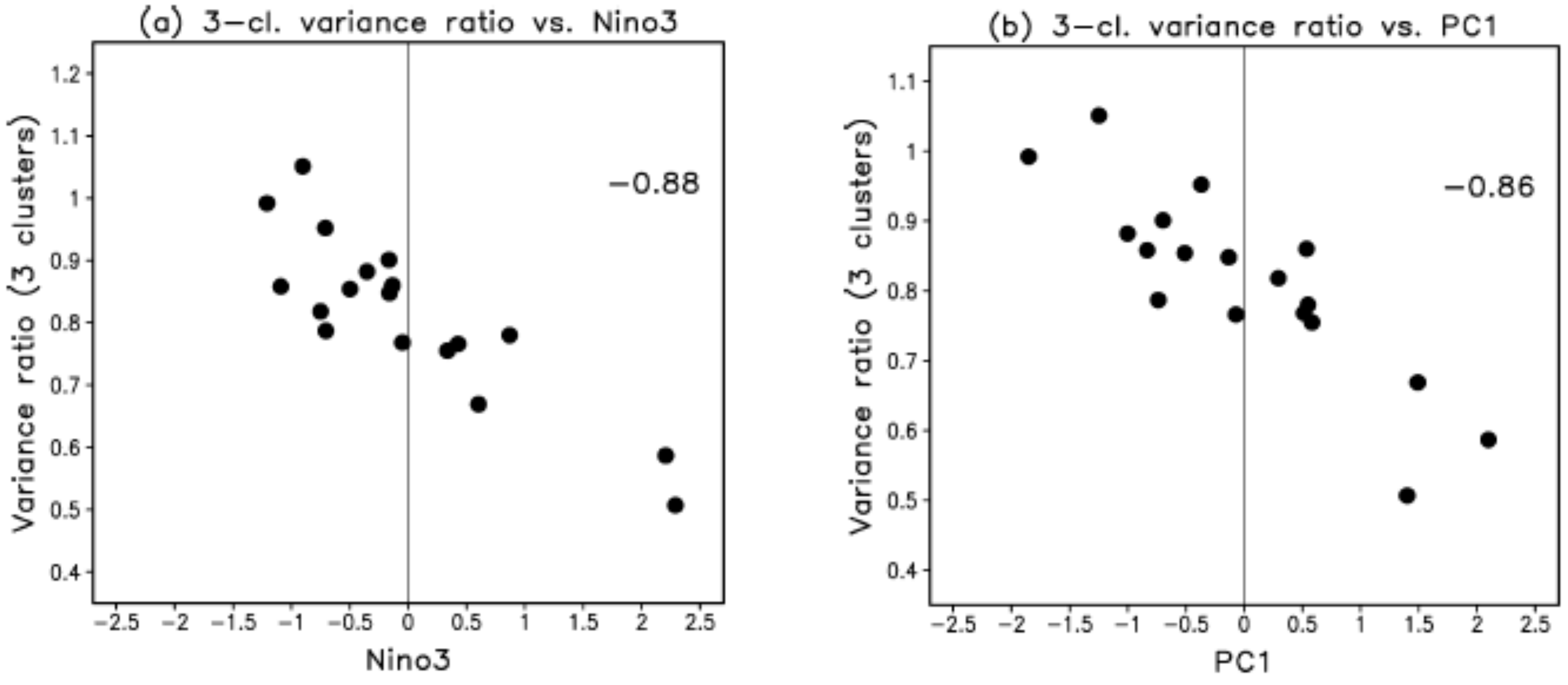

FIG. 4. Scatterplots of (a) the 3-cluster ($k = 3$) variance ratio vs Niño-3, and (b) the 3-cluster variance ratio vs the leading PC of ensemble/seasonal means. The leading PC and SST index time series are standardized.

Sub-seasonal variability: the Madden-Julian Oscillation (MJO)

Wheeler – Hendon (2004) MJO metric based on composite EOFs

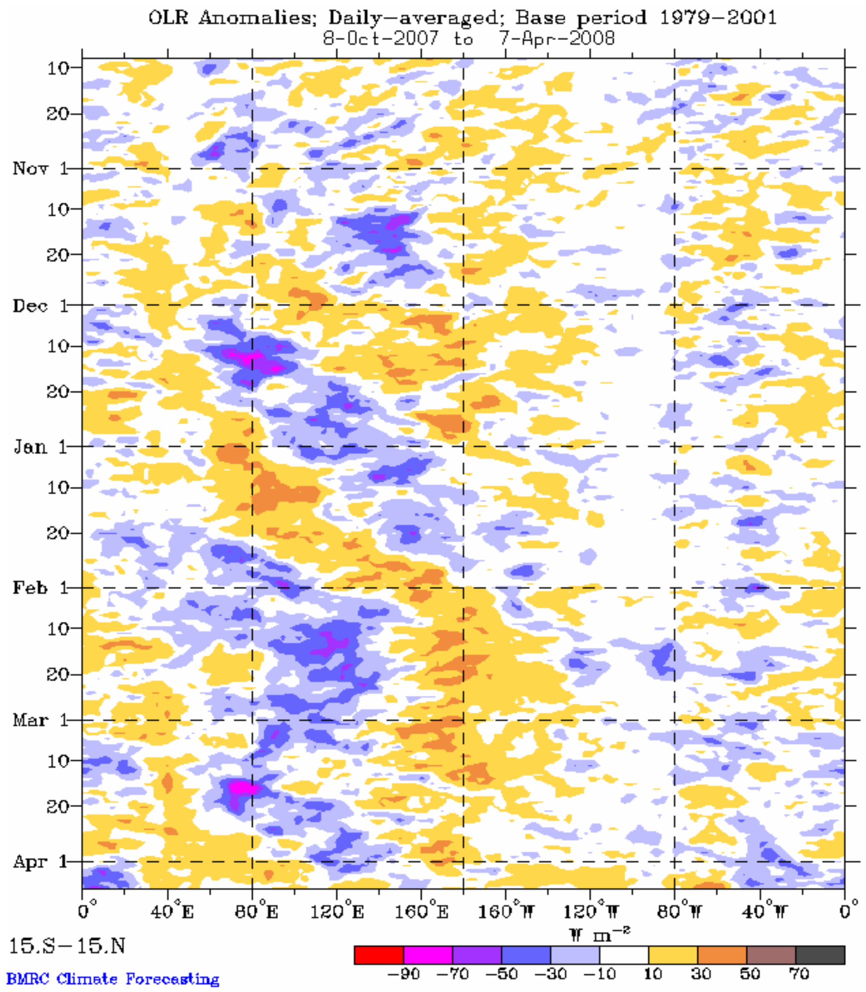

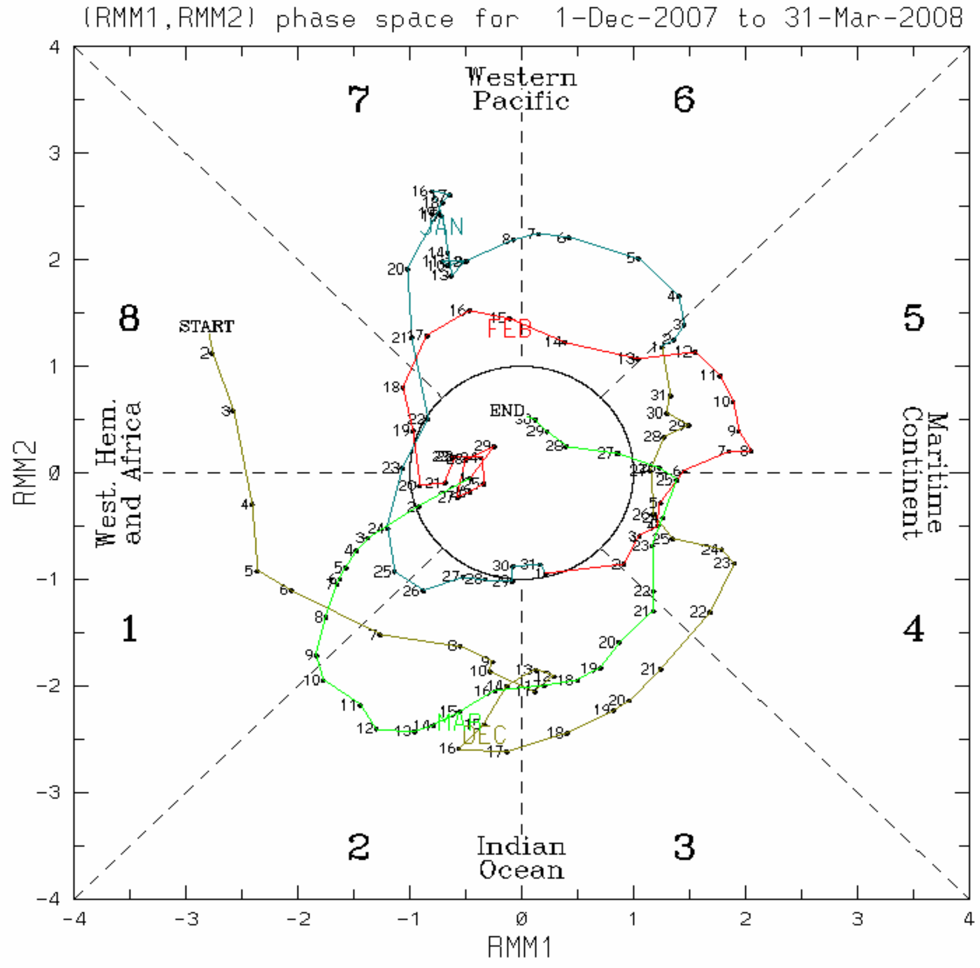

Impact of MJO on Euro-Atlantic regimes

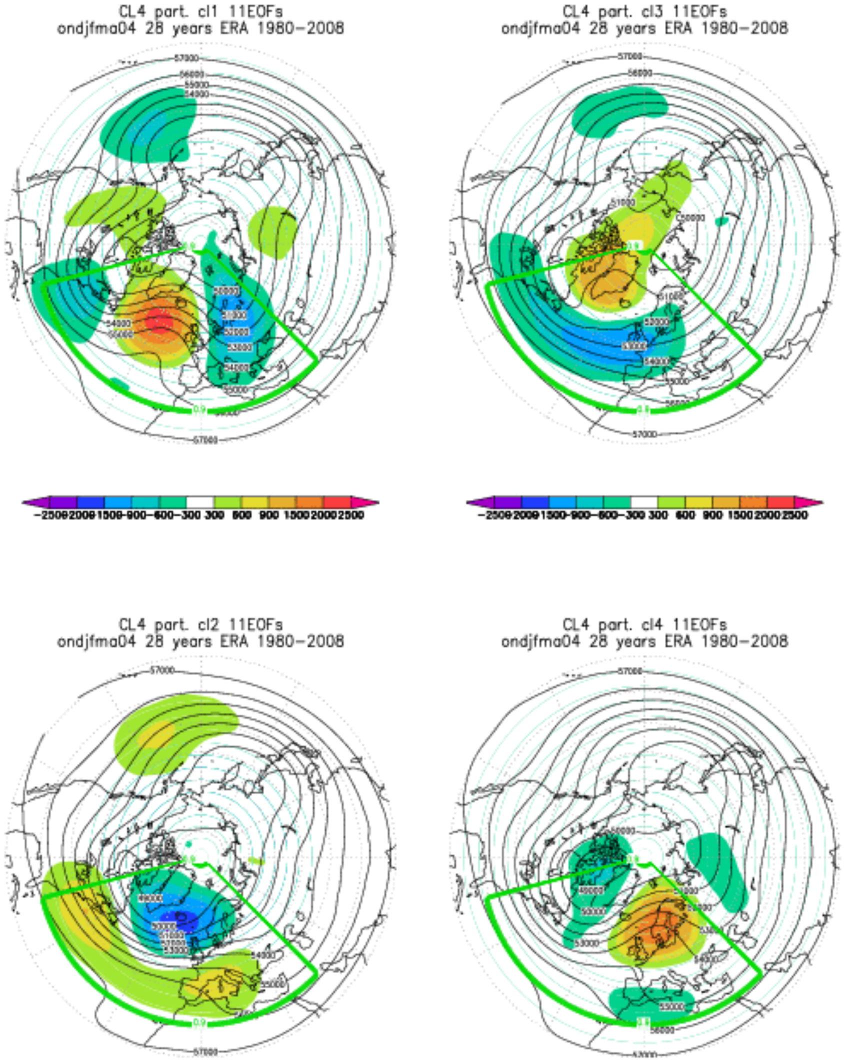

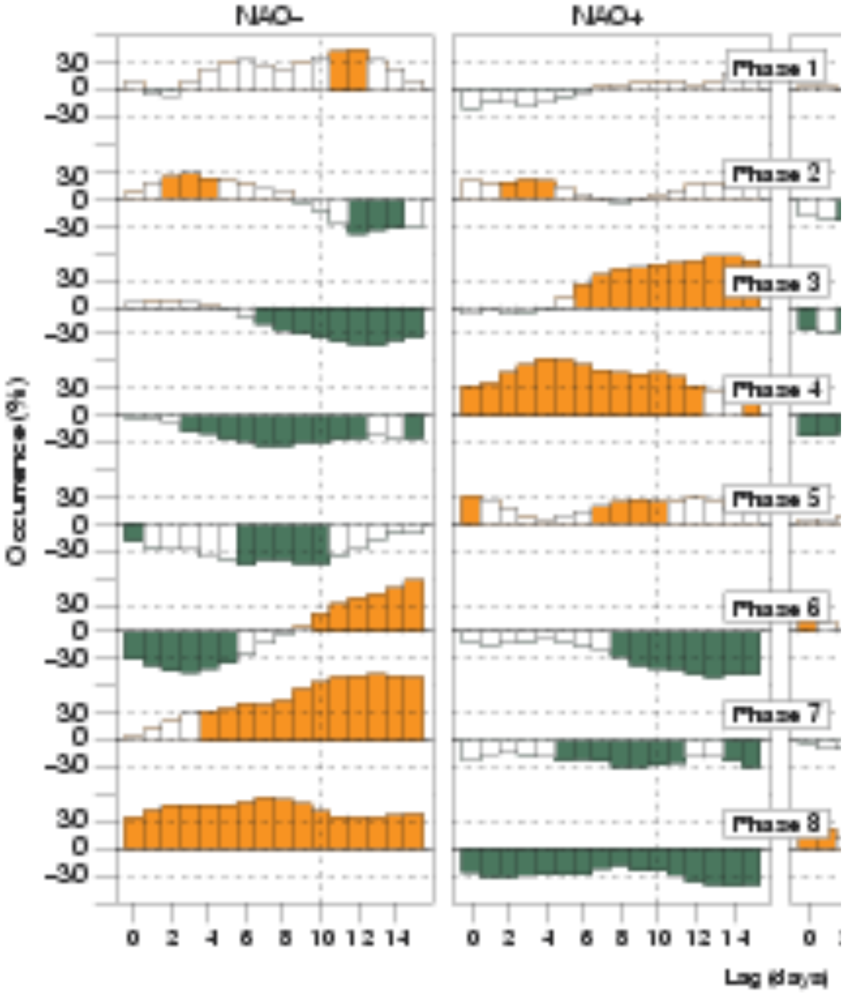

Cassou 2008

Summary

- Flow regime behaviour can be reproduced in a variety of dynamical models of different complexity.
- Atmospheric flow regimes may be defined on a hemispheric or regional domain.
- Detection of regimes in atmospheric and model datasets is usually performed by PDF estimation or cluster analysis; results are dependent on adequate time-filtering and proper use/interpretation of statistical significance tests.
- The impact of forcing anomalies on regime properties may occur through changes in regime frequencies or bifurcation effects.
- Predictability of regime frequencies and variations in the number of regimes as a function of the ENSO and MJO phases have been detected in ensembles of GCM simulations, and offer an alternative approach to long-range prediction.

Flow regimes over the North Atlantic and teleconnections with the tropics

Franco Molteni

ECMWF, Reading, U.K.

ECMWF

Outline

- A comparison of regimes obtained from cluster analysis over different NH domains: are Atlantic and Pacific regimes connected?
- Impact of tropical heating over the Indian – West Pacific ocean: modelling studies on decadal and sub-seasonal scales
- Teleconnections with Indo-Pacific rainfall from GPCP data and ECMWF re-analyses
- Impact of Atlantic and Pacific regimes on surface heat fluxes over the northern oceans
- The role of the stratosphere

EOF & cluster analysis in three NH domains

Data: 5-day means of Z 500 hPa in DJF 1979/80 to 2012/13 (from ERA-interim)

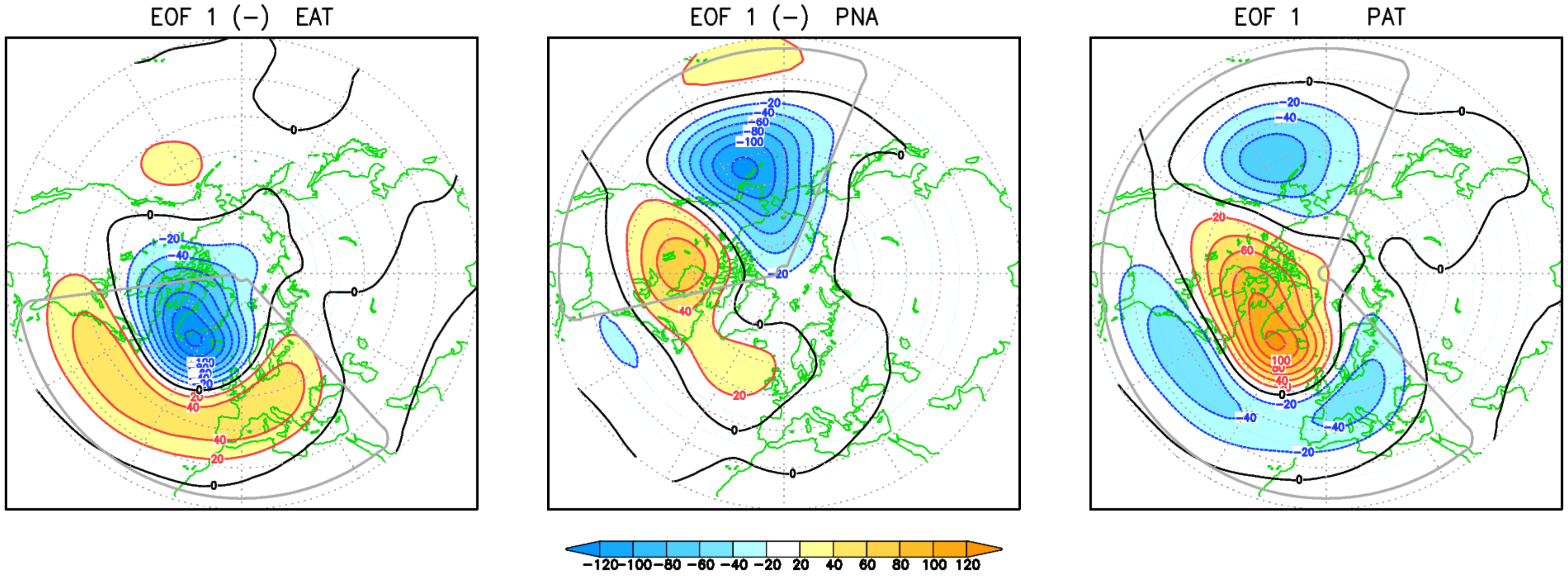

Cluster analysis method: k-means
(Michelangeli et al. 1995, Straus et al. 2007)

Euro-Atlantic 4-cluster centroids

NAO+
31.5%

Blocking
25.0%

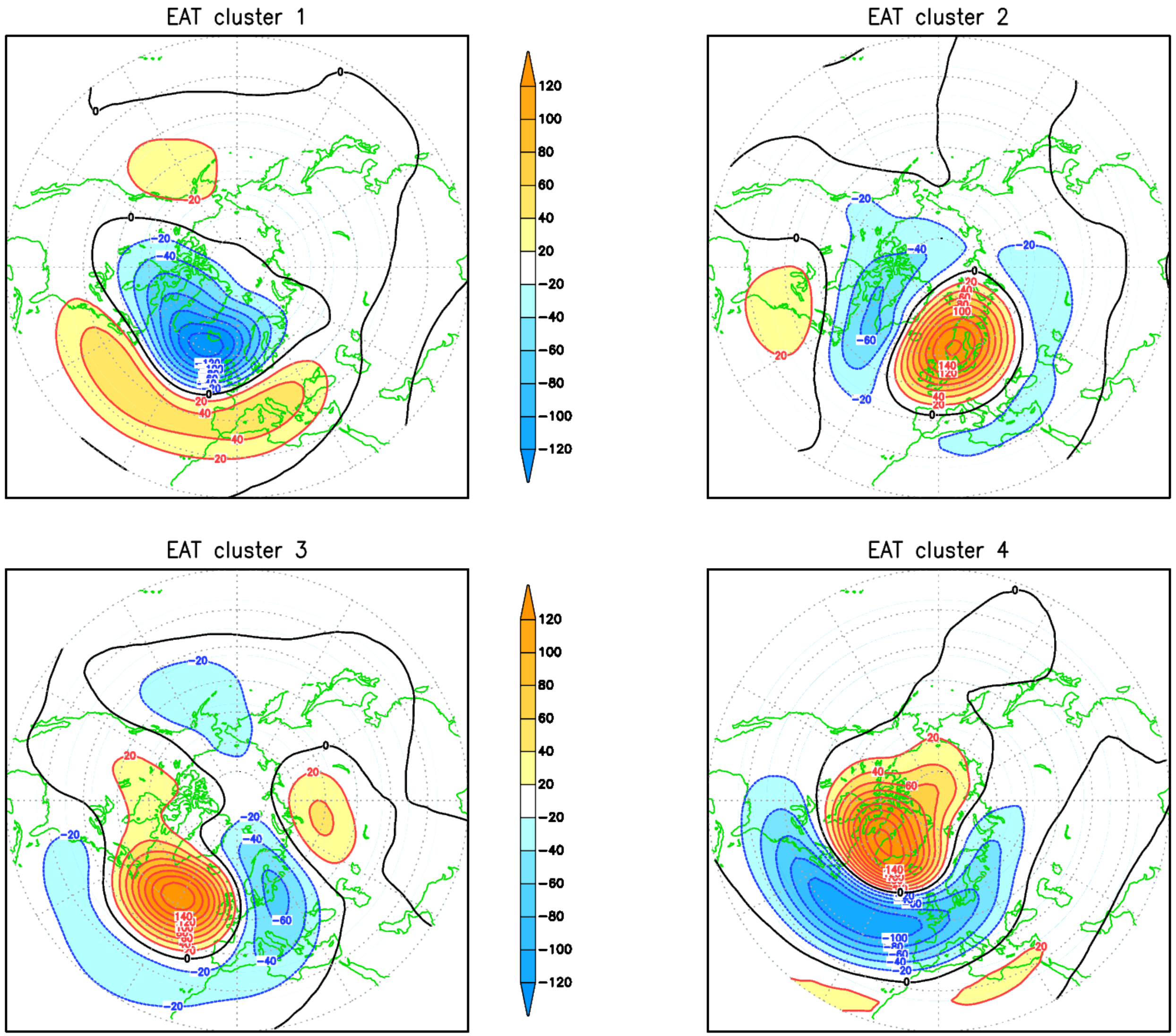

Atl. Ridge
22.2%

NAO-
21.3%

Pacific-North American 4-cluster centroids

Pacific Trough
27.7%

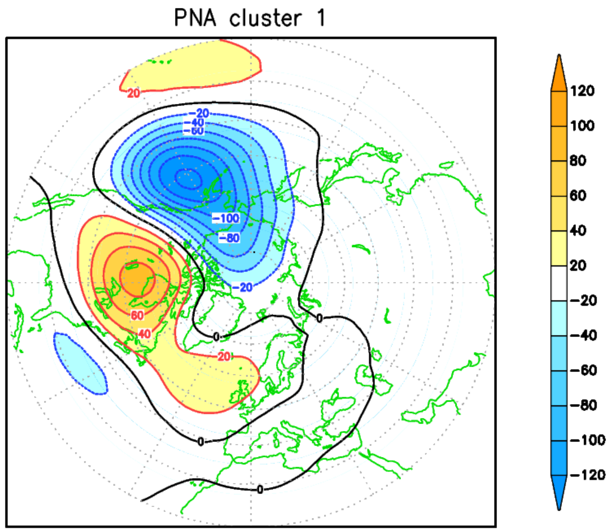

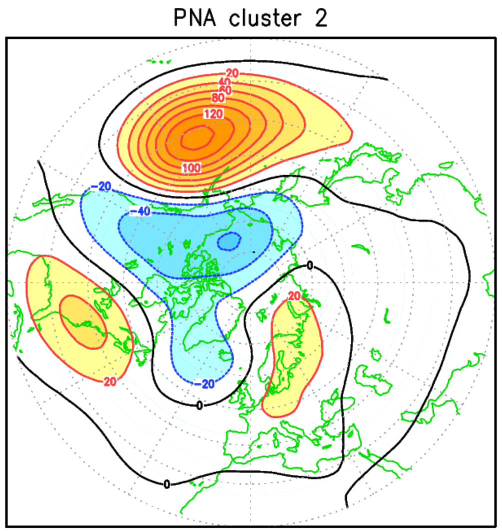

Arctic Low
(PNA-)
27.7%

PNA+
24.0%

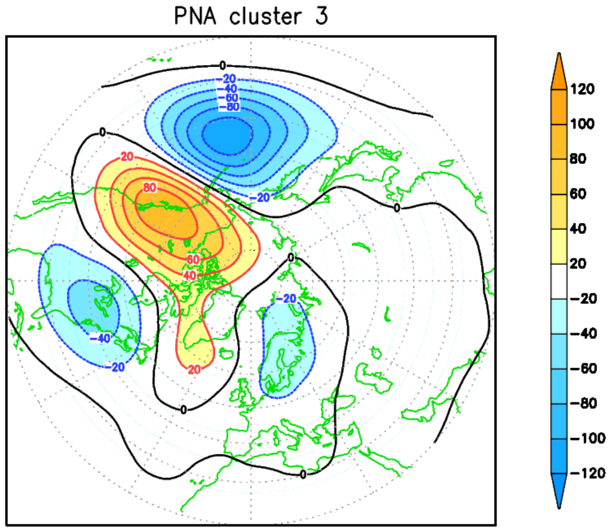

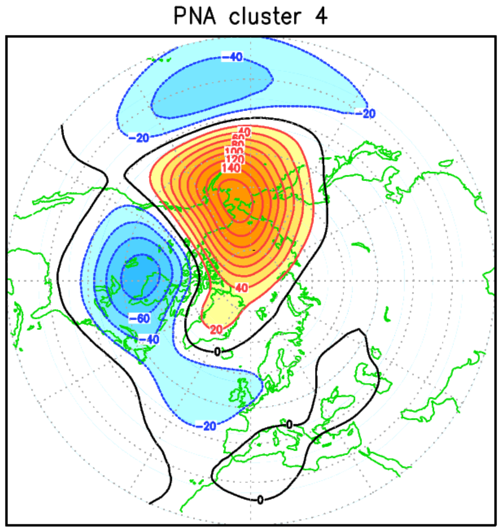

Alaskan
Ridge
20.6%

Centroid of the most populated cluster

EAT cluster 1

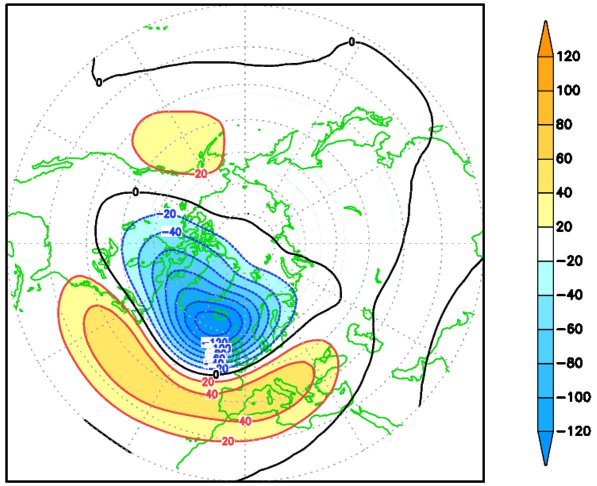

PNA cluster 1

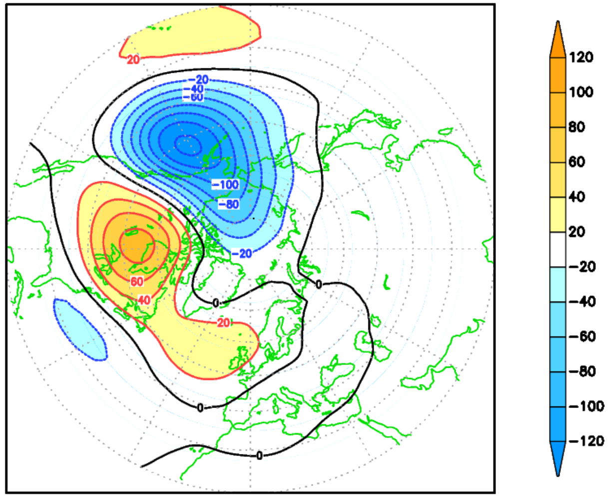

PAT cluster 1

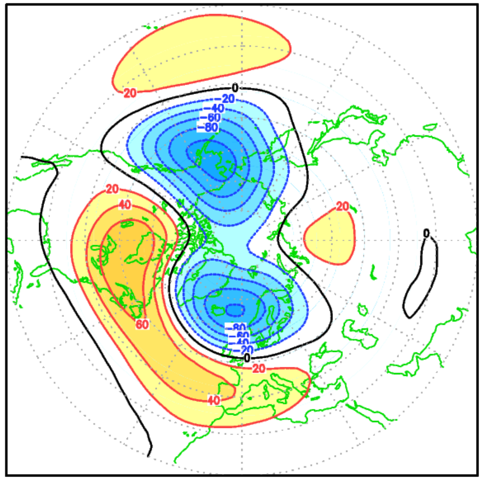

NAO+ 31.5%

Pac Trough 27.7%

COWL 18.8%

EOF 1 (–) EAT

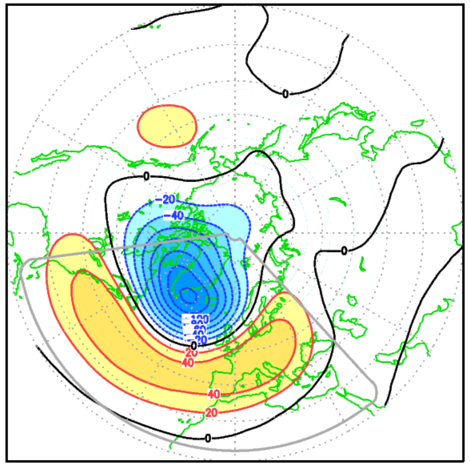

EOF 1 (–) PNA

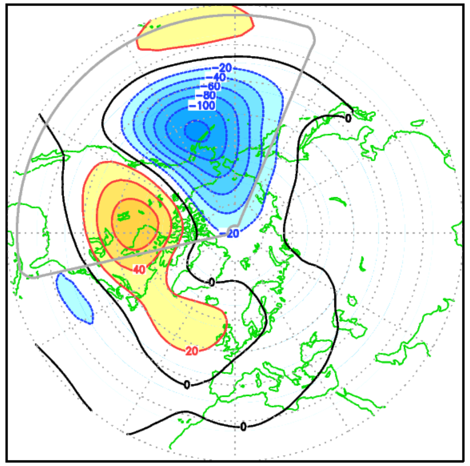

EOF 1 PAT

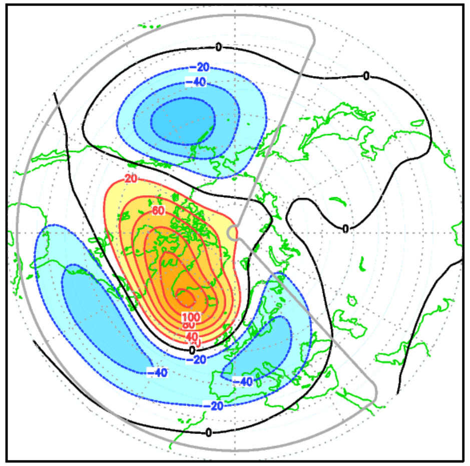

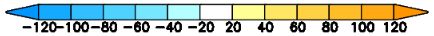

AGCM exp: late 20th cen. trends, Hurrell et al. 2004

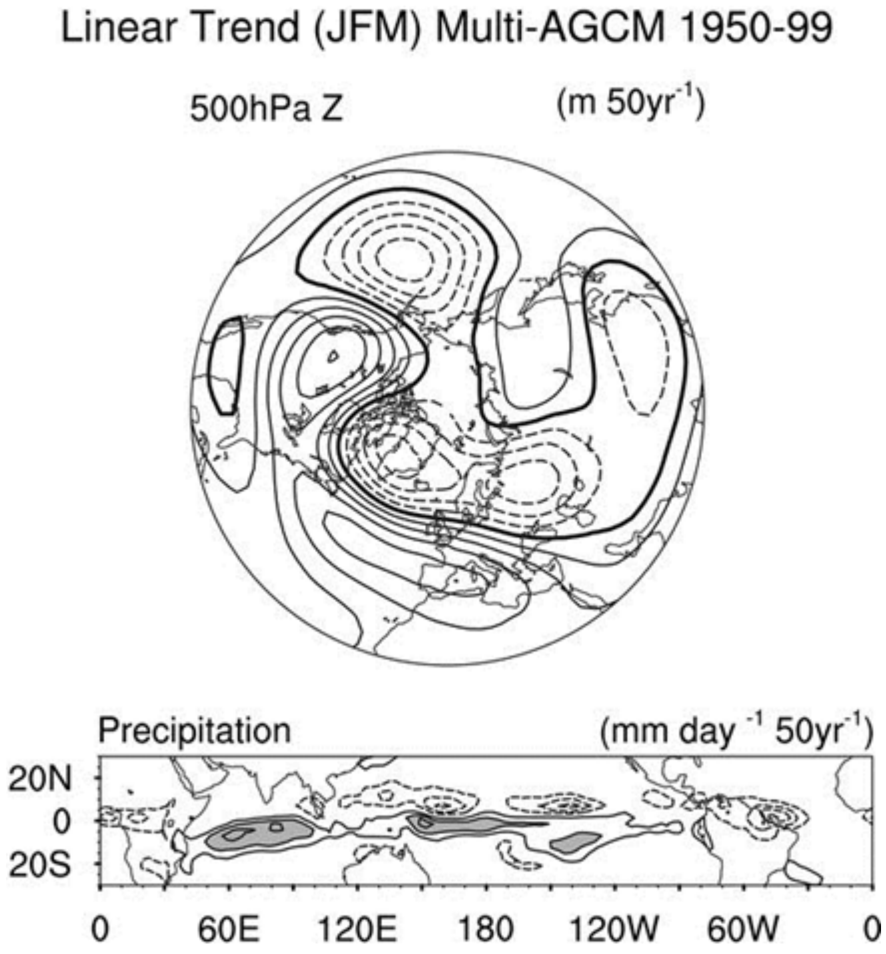

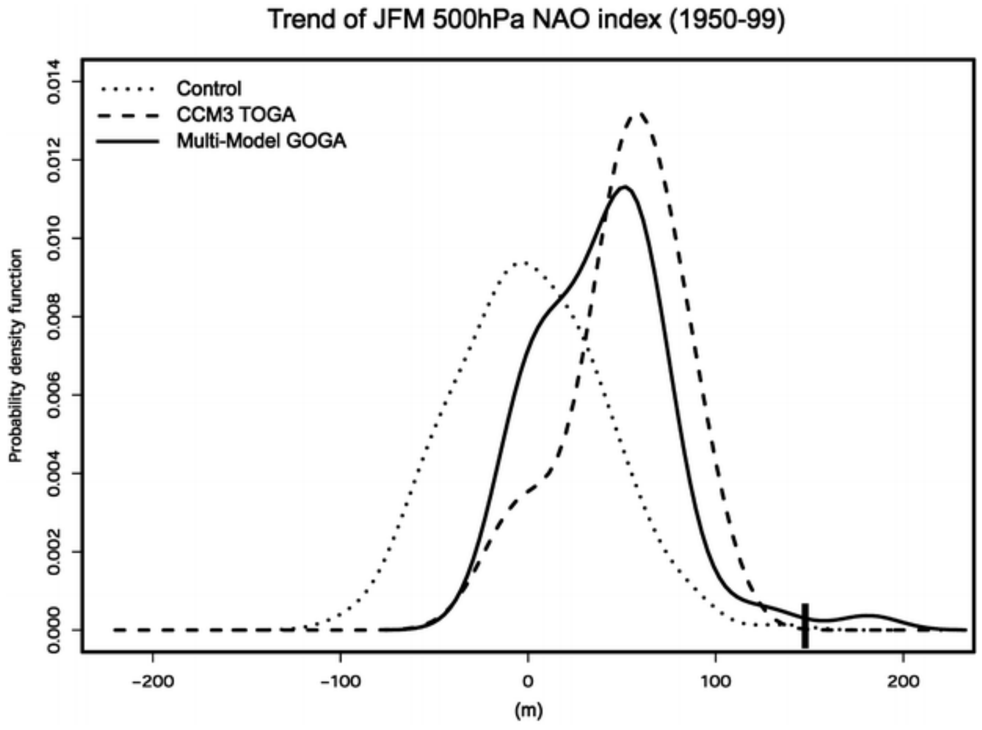

JFM NAO index

AGCM exp: late 20th cen. trends, Hoerling et al. 2004

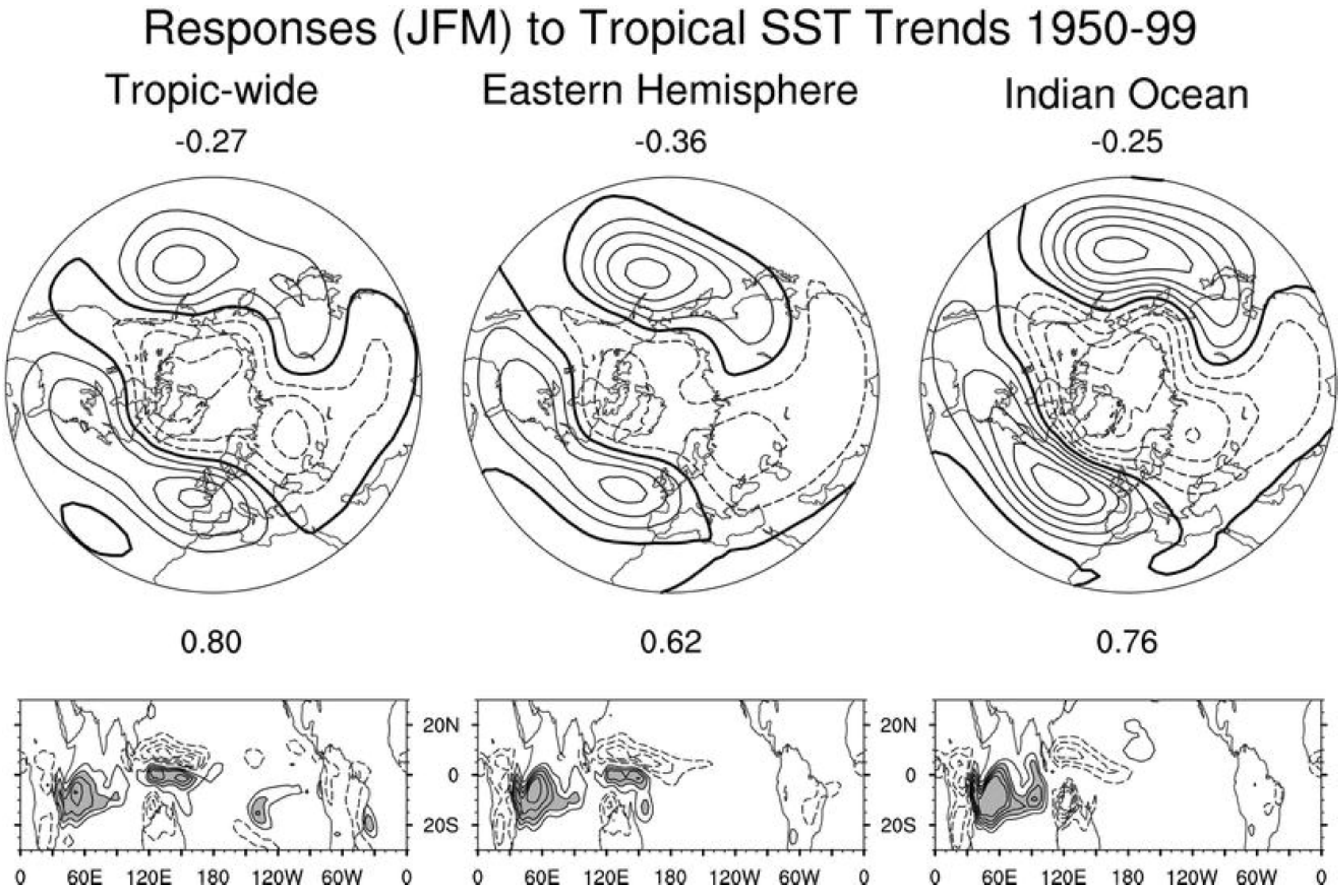

CCM3

Z 500

Prec.

Impact of the MJO on the NH extra-tropics: composites from ERA-int.

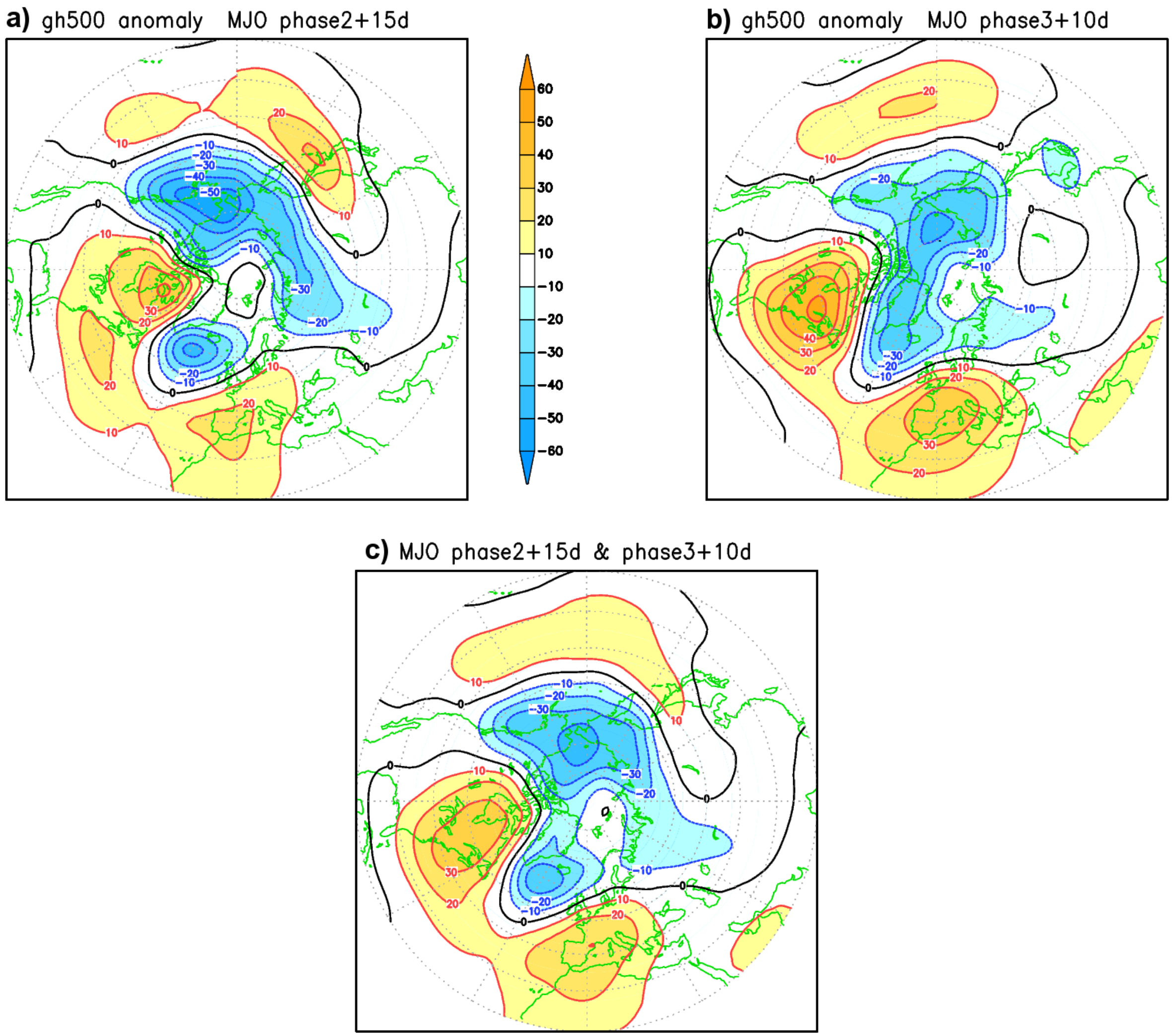

Impact of the MJO on the NH extra-tropics

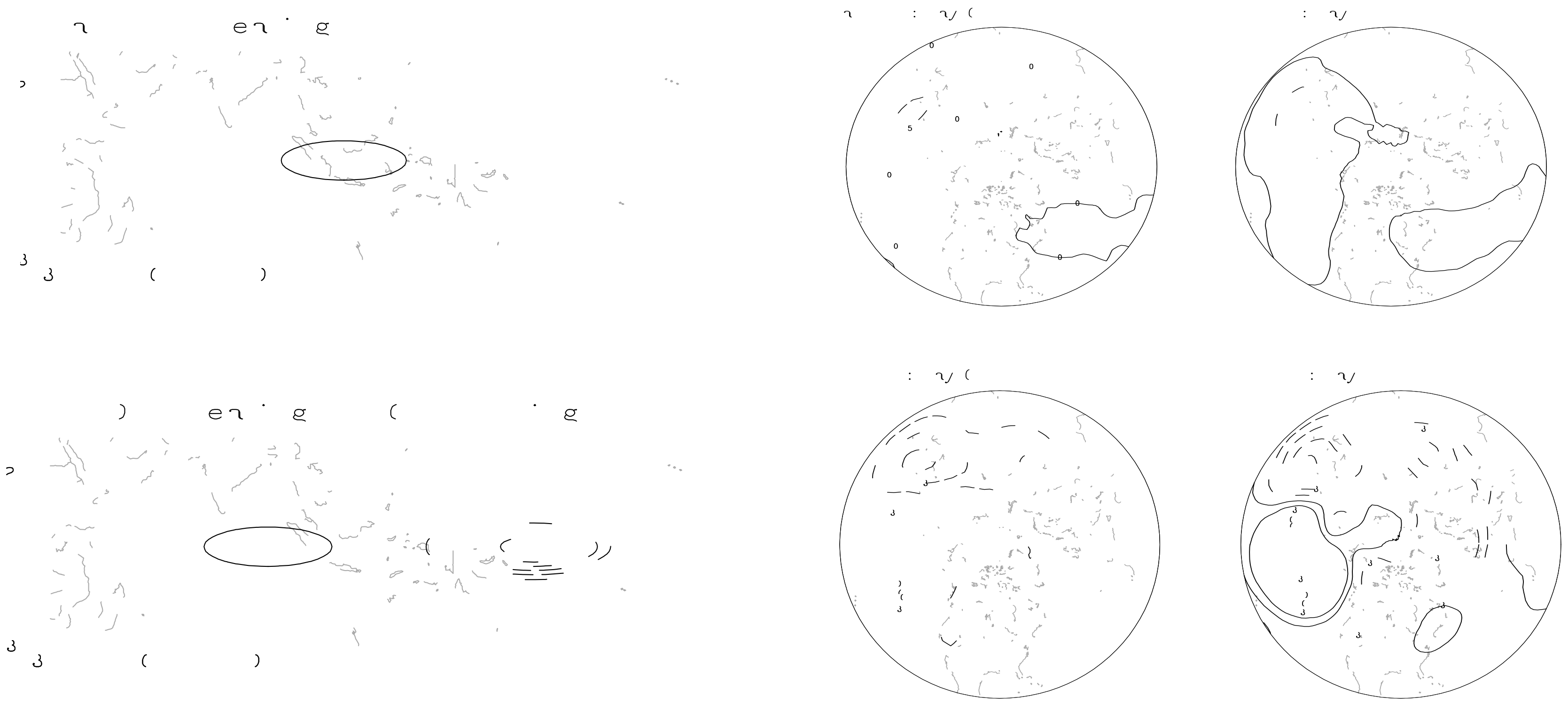

Lin et al, MWR 2010

See also

Simmons et al JAS 1983

Ting and Sardeshmukh JAS 1993

Teleconnections from Indian Ocean & W. Pacific in DJF

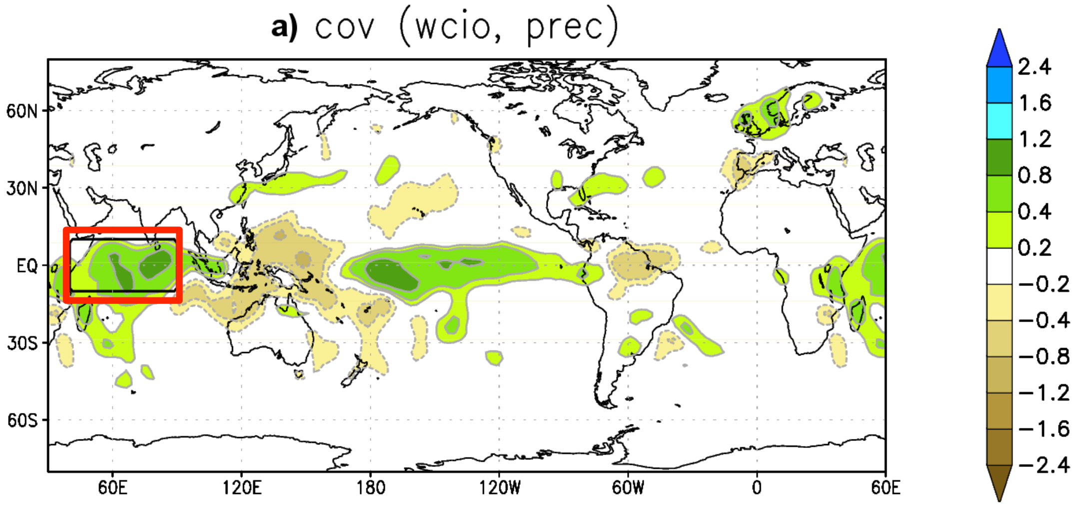

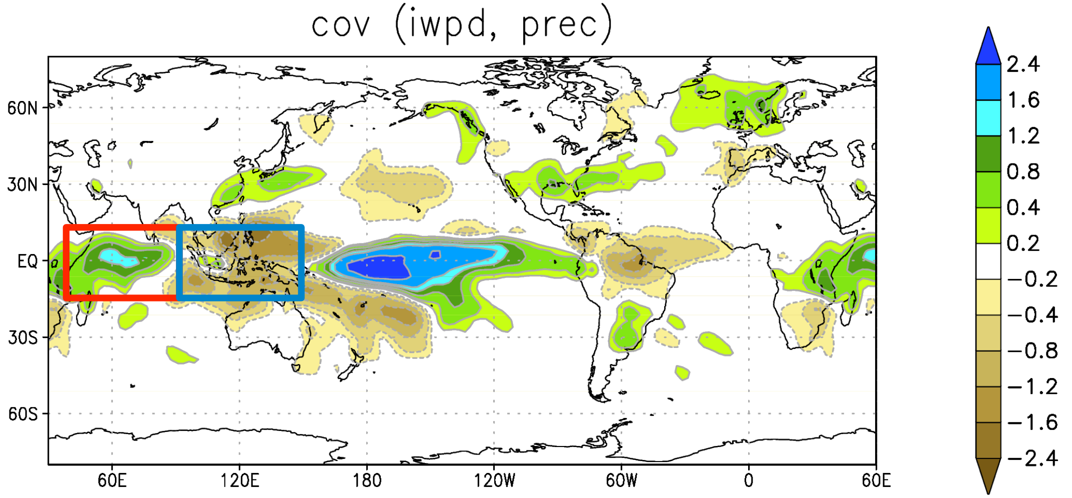

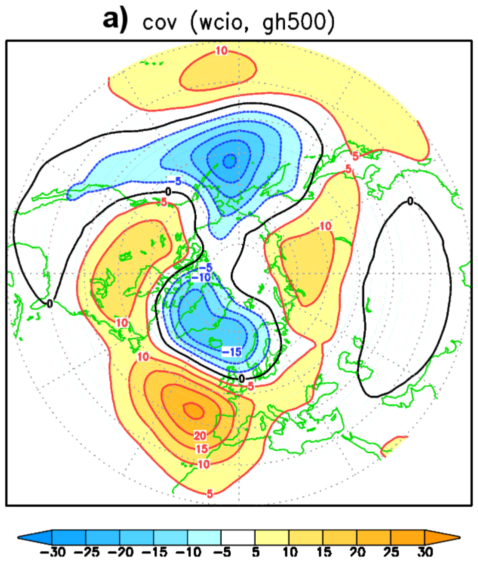

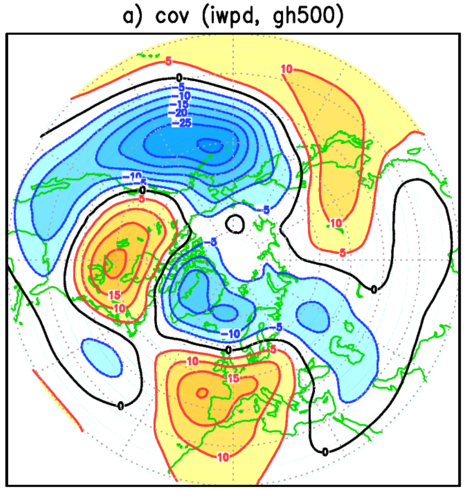

Molteni, Stockdale, Vitart
ClimDyn 2015

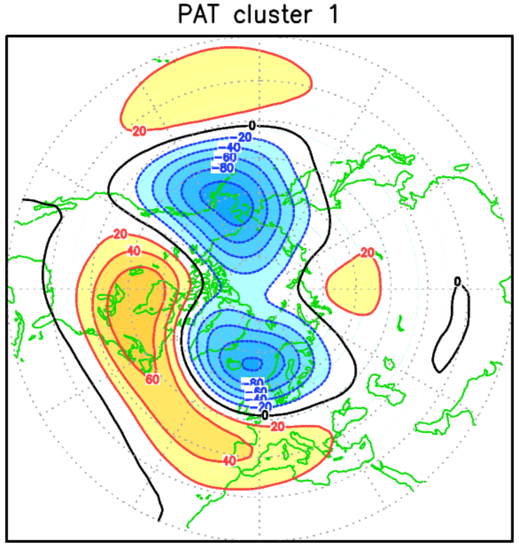

Teleconnections from Indian Ocean & W. Pacific in DJF

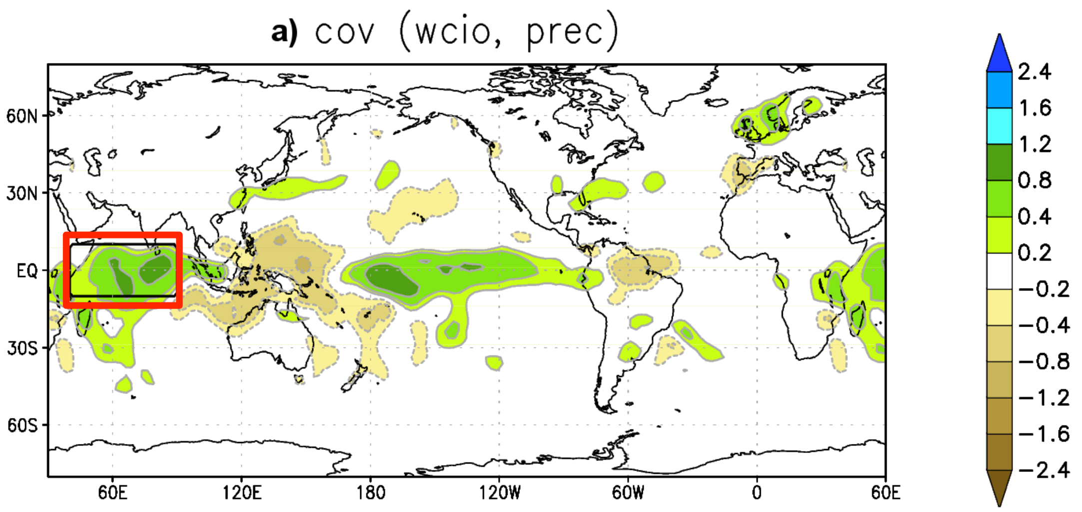

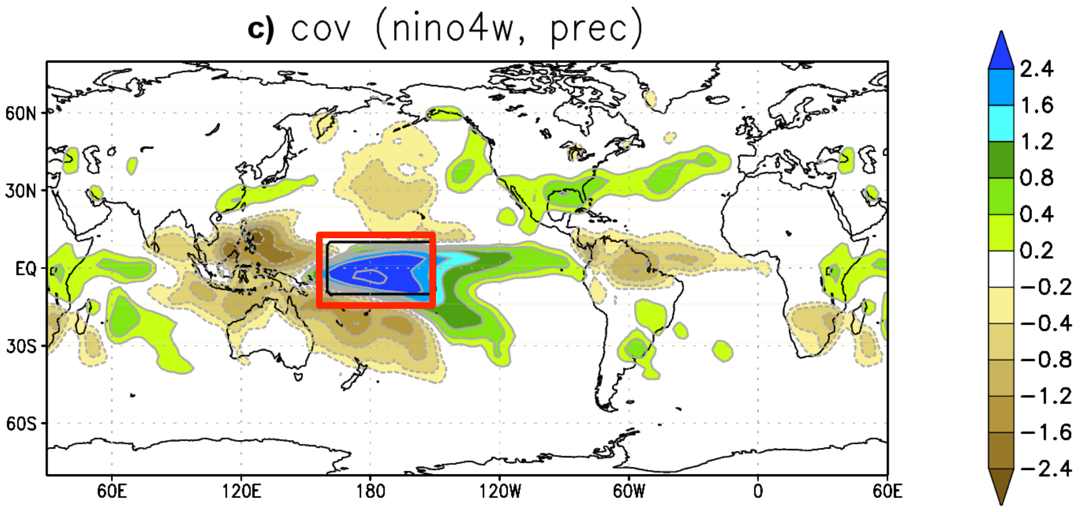

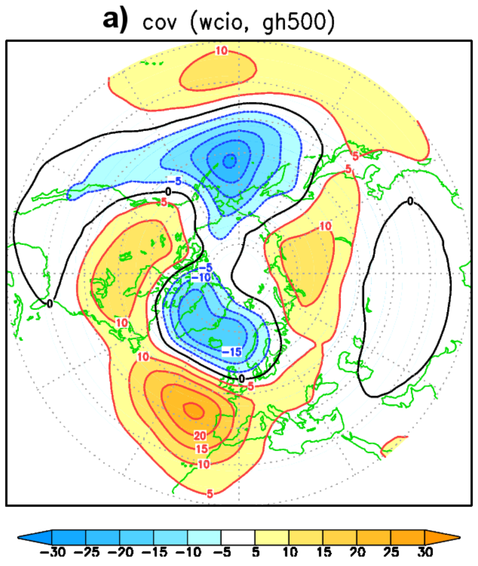

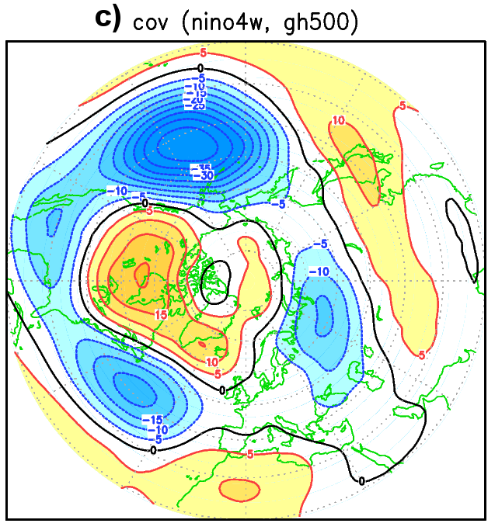

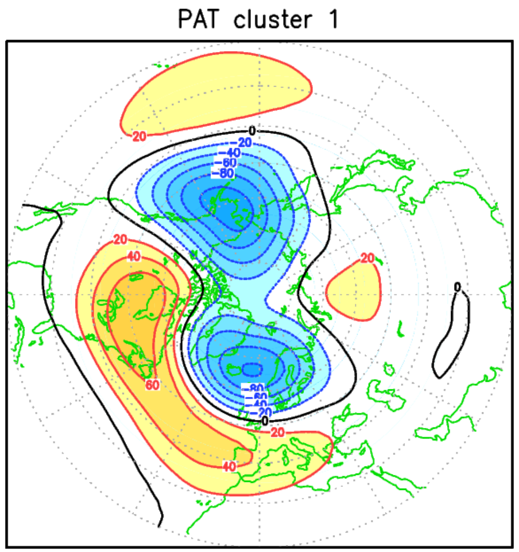

Covariances with W. Indian Ocean rainfall in CERA20C

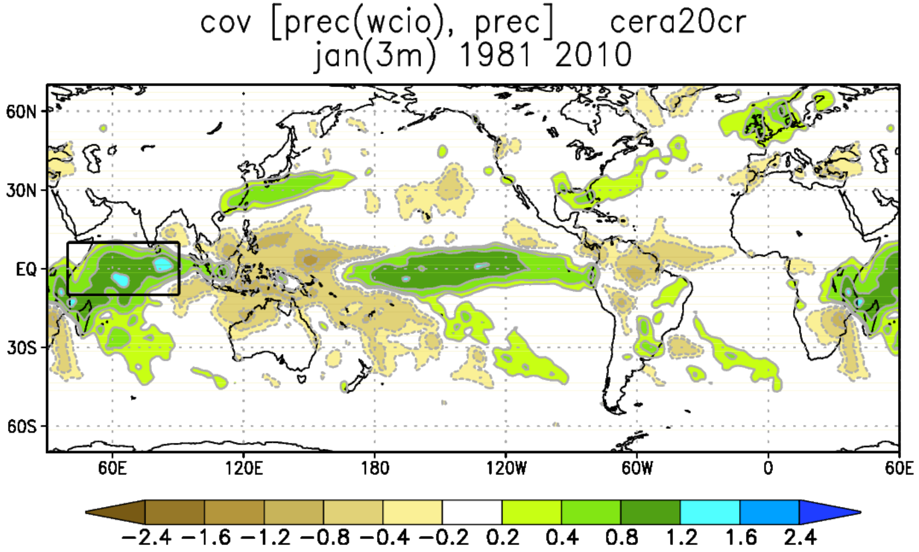

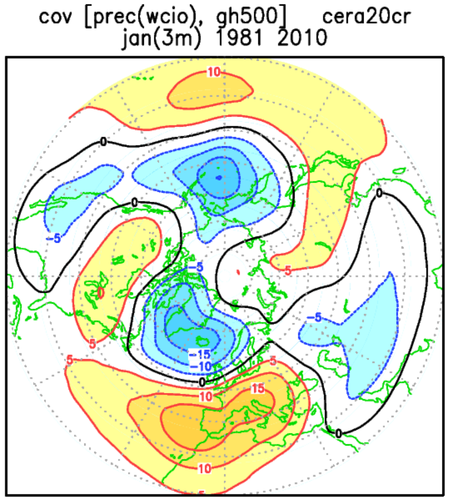

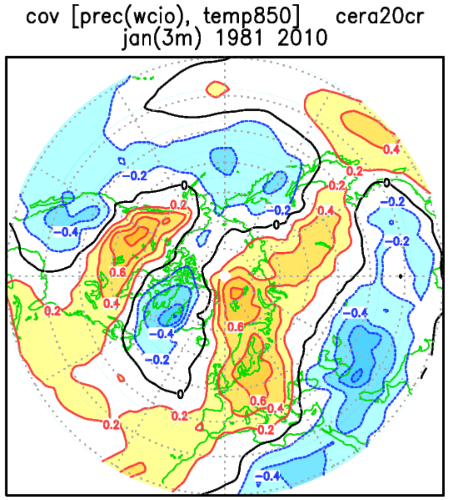

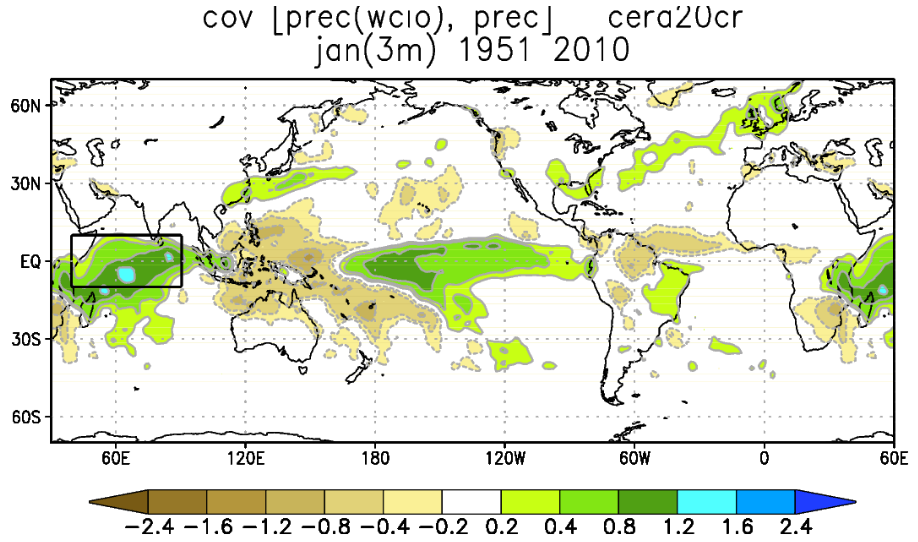

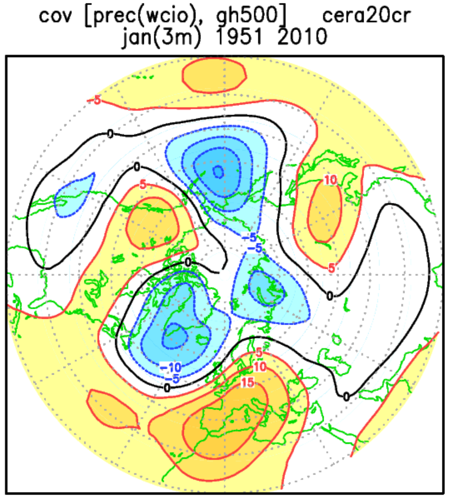

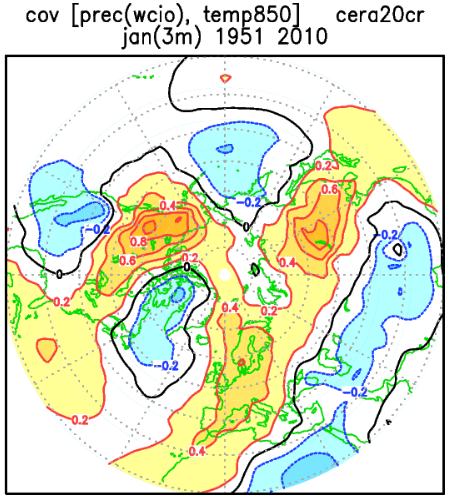

Teleconnections and multi-decadal variability in CERA20C

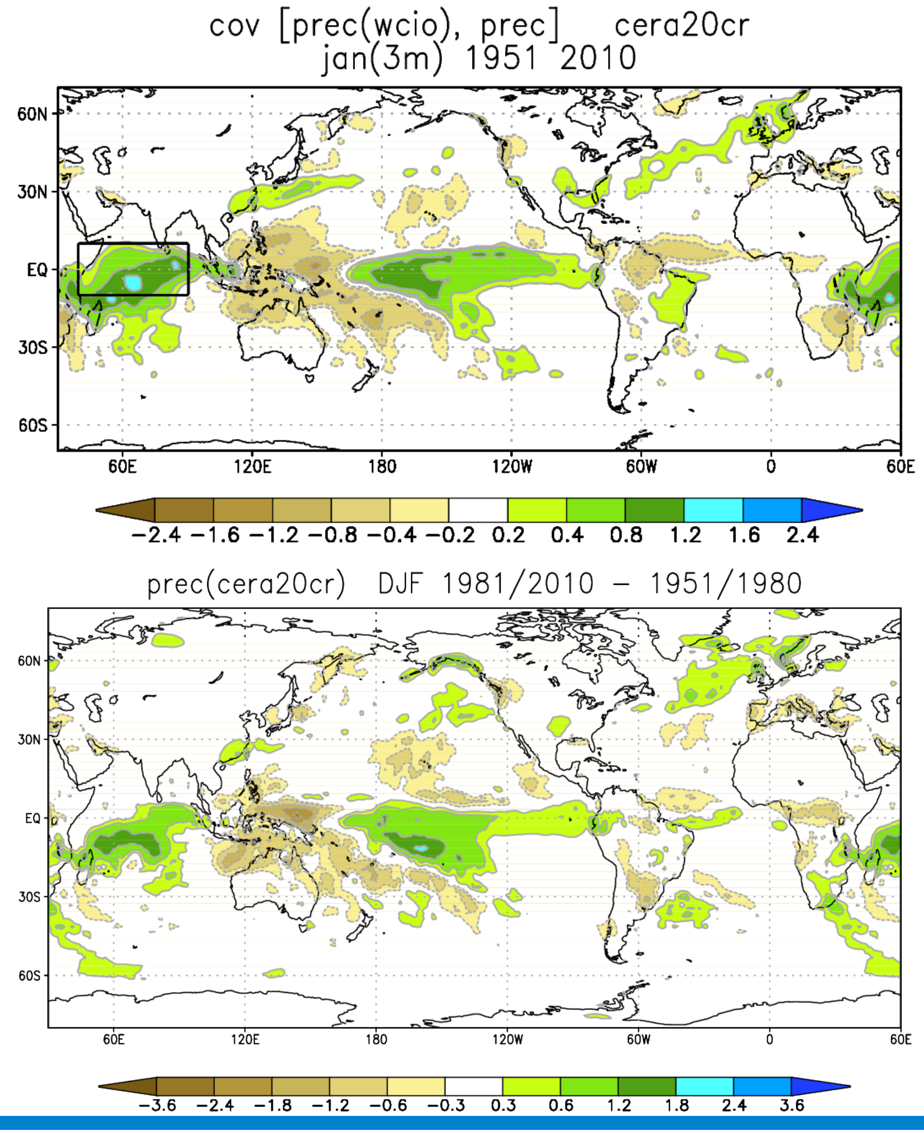

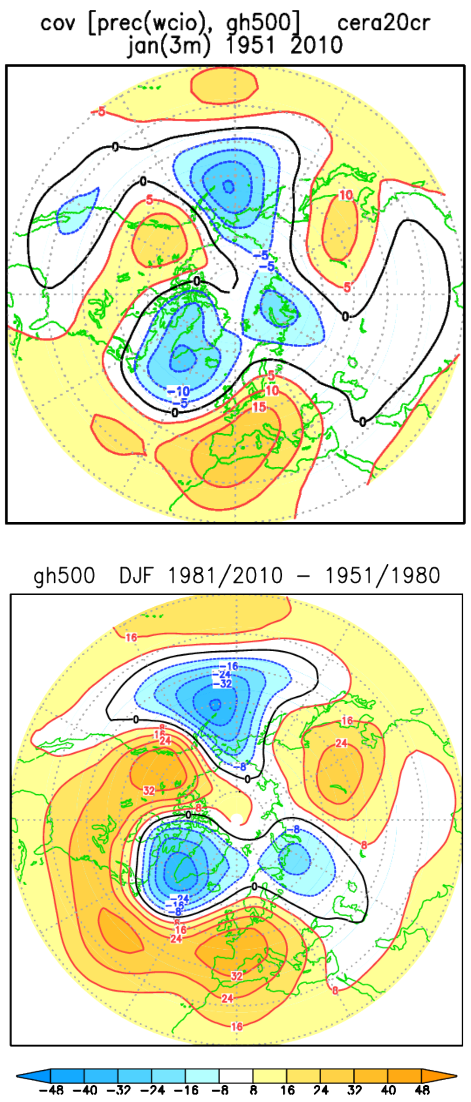

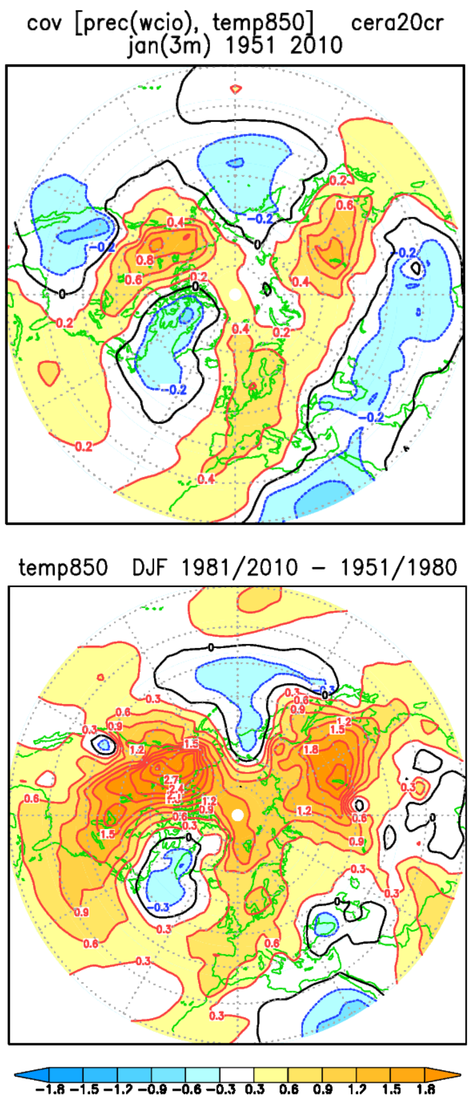

Modelling decadal variability on near-surface temperature trends

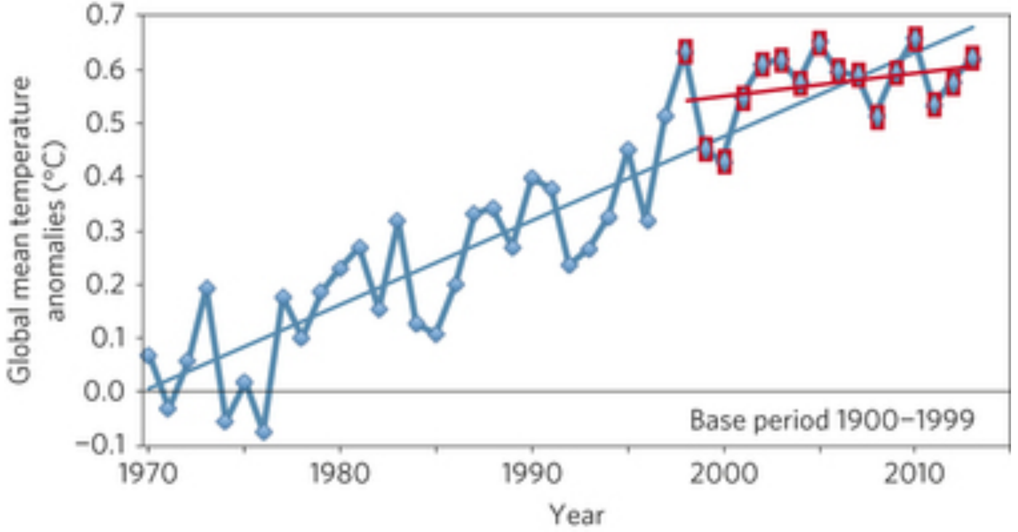

Kosaka and Xie (Nature 2013):

"pacemaker" experiment for 2002-2012

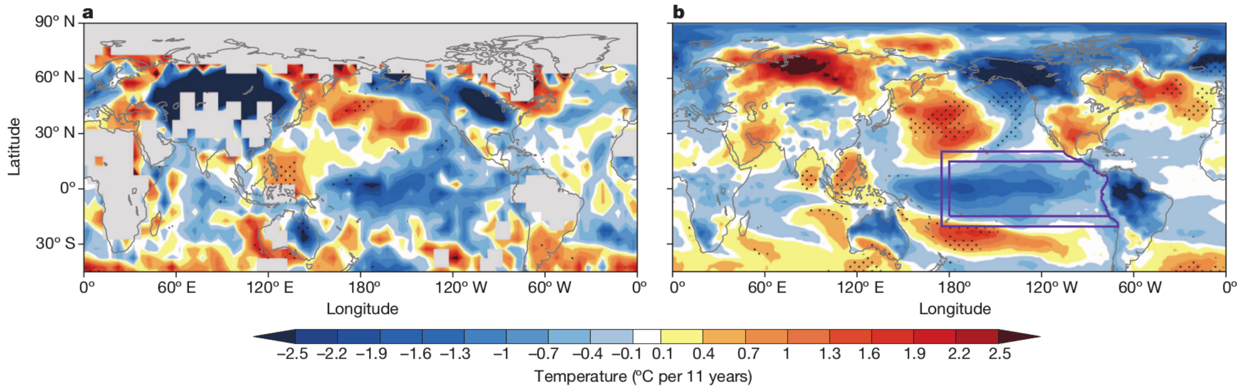

Linear trends from HadCRUT:

1984-1998: 0.26 °C/decade

1998-2012: 0.04 °C/decade

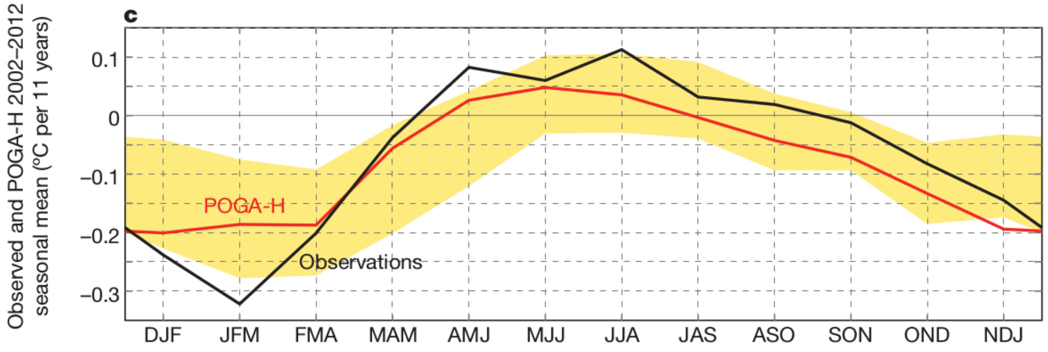

st.dev. of annual–mean non–solar heat flux
ERA–interim 1979–2013

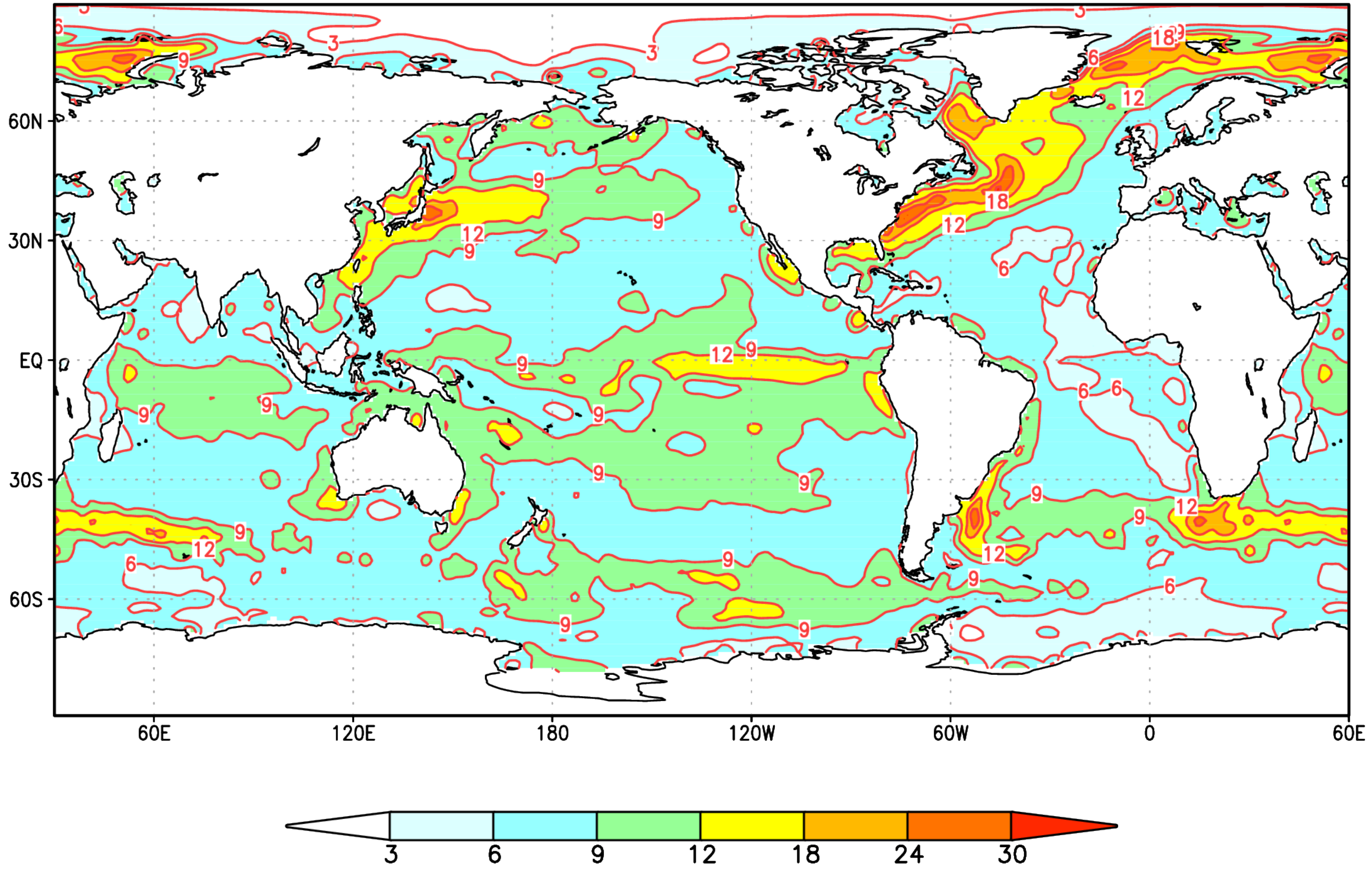

Spread in the magnitude of climate model interdecadal global temperature variability traced to disagreements over high-latitude oceans

Patrick T. Brown[1], **Wenhong Li**[1], **Jonathan H. Jiang**[2], **and Hui Su**[2]

[1]Earth and Ocean Sciences, Nicholas School of the Environment, Duke University, Durham, North Carolina, USA, [2]Jet Propulsion Laboratory, California Institute of Technology, Pasadena, California, USA

Abstract: … efforts to constrain the climate model produced range of unforced interdecadal variability in global SAT would be best served by focussing on air-sea interactions at high latitudes.

Key Points:

- Climate models show substantial disagreement on the magnitude of natural global mean surface temperature variability
- The spread in the simulated magnitude of global temperature variability is not due to model disagreement over the tropical Pacific
- The spread in the simulated magnitude of global temperature variability is linked strongly to model disagreement over high-latitude oceans

Drivers of uncertainty in simulated ocean circulation and heat uptake

Markus B. Huber[1] **and Laure Zanna**[1]

[1]Department of Physics, University of Oxford, Oxford, UK

Abstract: … This study demonstrates that model biases in air-sea fluxes are one of the key sources of uncertainty in climate simulations.

Key Points:

- Ocean model is forced with air-sea fluxes from CMIP5 models to examine the drivers of uncertainty in ocean circulation and heat uptake (OHU)
- High-latitude air-sea fluxes are the dominant source of uncertainty in the spread of Atlantic MOC and OHU over model structural uncertainty
- Subgrid-scale parameters lead to large uncertainty in the circulation and OHU, especially in the Pacific and Southern Oceans

Co-variability of NH ocean heat fluxes and circulation anomalies

Thermal forcing
Wave index (TW)
in DJF 1982 – 2011

Positive =
Increased heat flux
from oceans to atm. in
40N-70N band

(Molteni et al. 2011,
2017)

inspired by theories on
thermal equilibration
of planetary waves:

Mitchell and Derome 1983
Shutts 1987
Marshall and So 1990

Covariance with TW
index in DJF
(from ERA-
interim):

Z 500 hPa

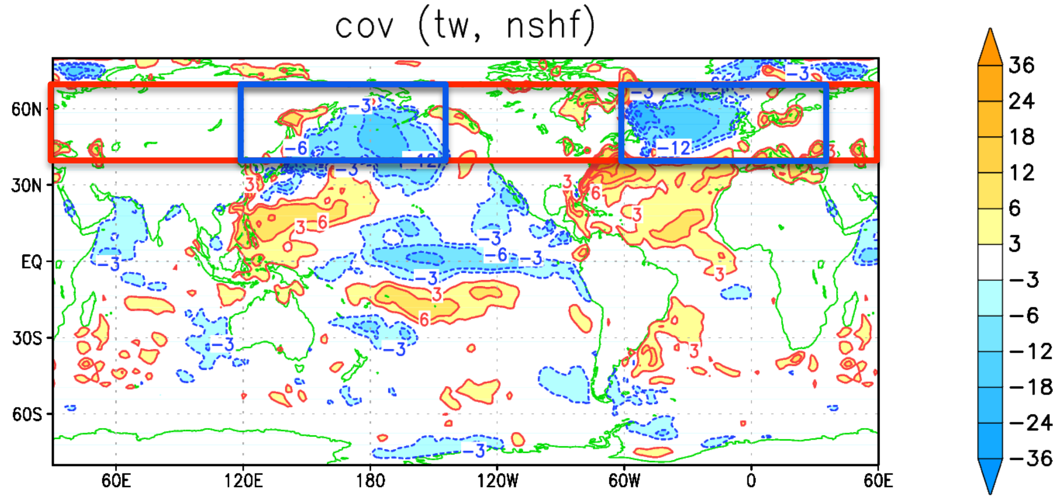

Net downward
surface
heat flux

Co-variability of NH ocean heat fluxes and circulation anomalies

Thermal forcing
Wave index (TW)
in DJF 1982 – 2011

Positive =
Increased heat flux
from oceans to atm. in
40N-70N band

(Molteni et al. 2011, 2017)

inspired by theories on
thermal equilibration
of planetary waves:

Mitchell and Derome 1983
Shutts 1987
Marshall and So 1990

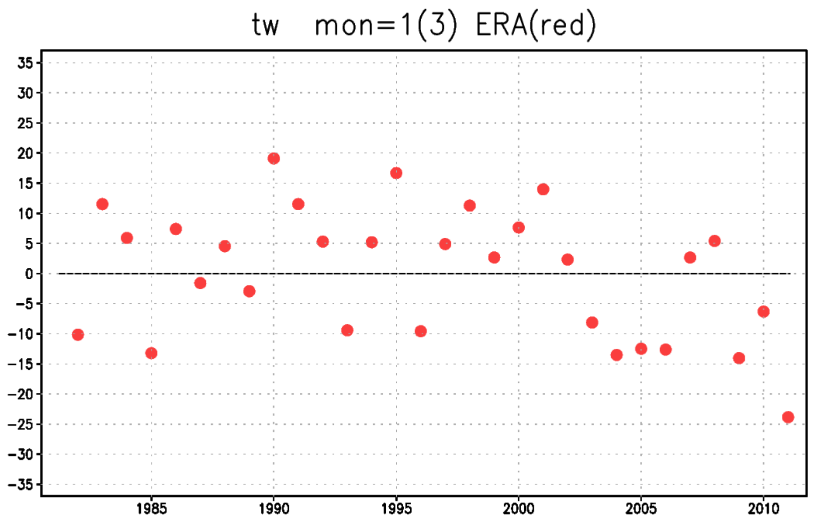

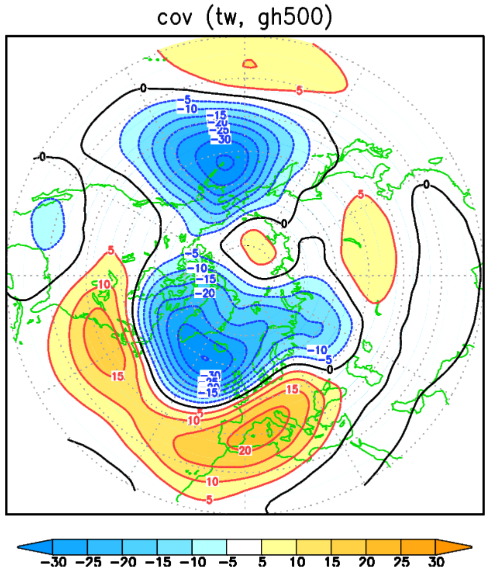

Covariance with TW index in DJF (from ERA-interim):

Z 500 hPa

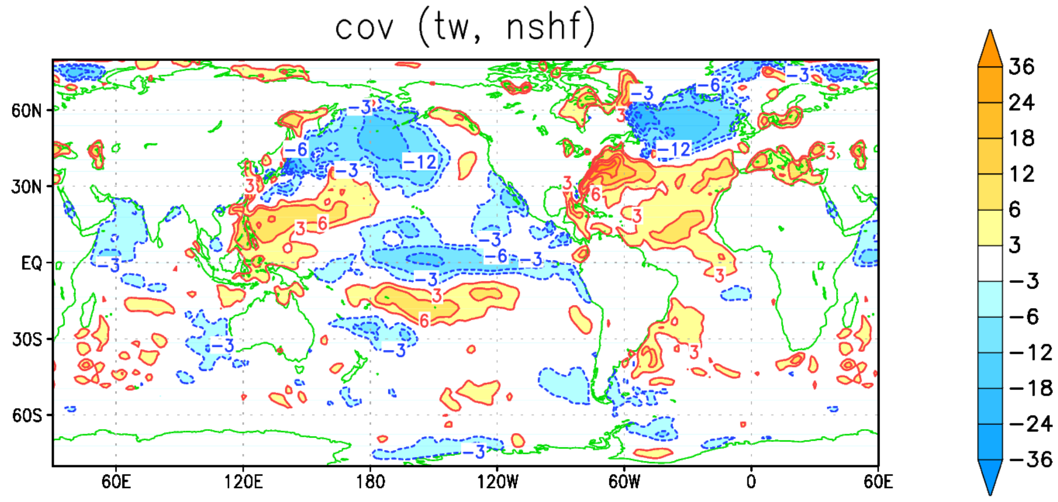

Net downward
surface
heat flux

NH heat flux co-variability with tropical Indo-Pacific rainfall

cov (iwpd, prec)

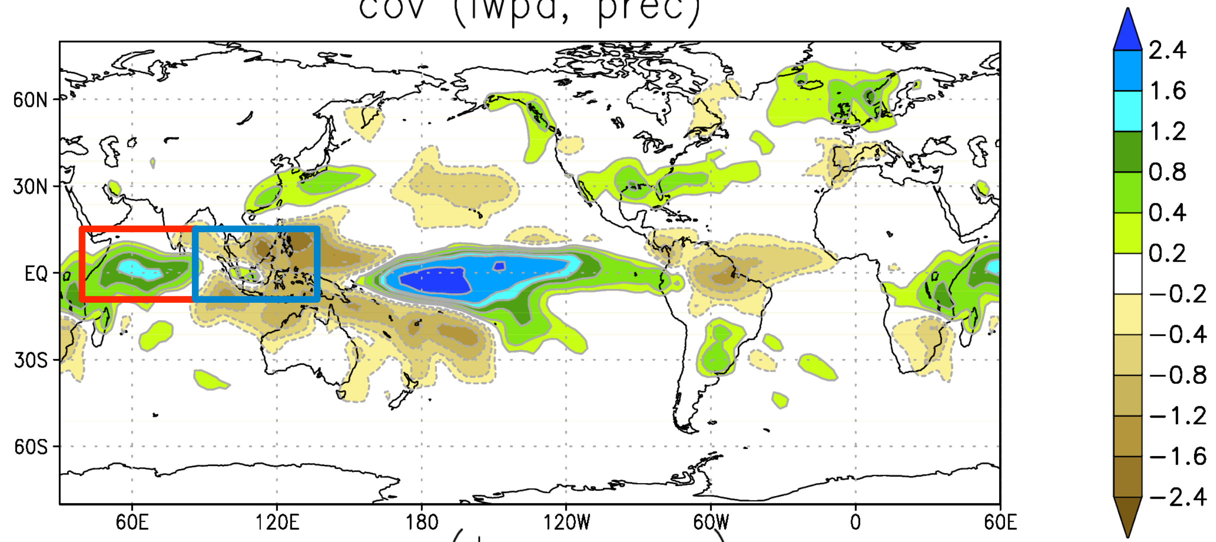

cov (tw, prec)

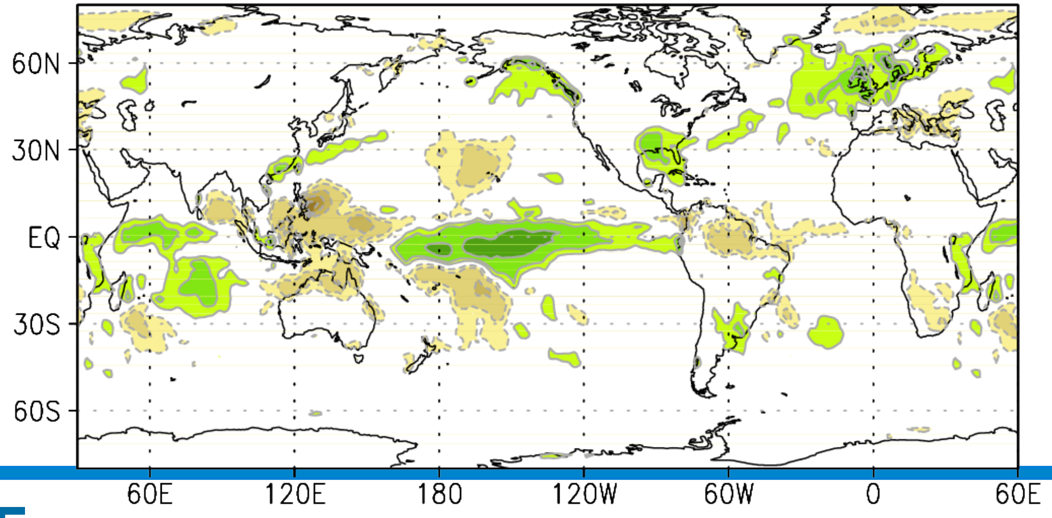

a) cov (iwpd, gh500)

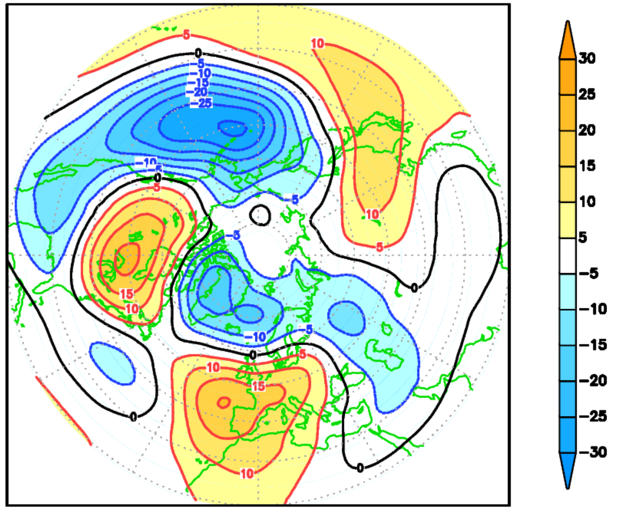

cov (tw, gh500)

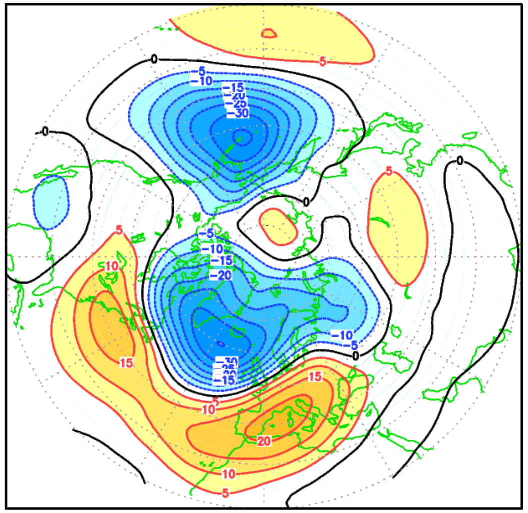

1st EOF of T 100 hPa in DJF and its covariance with Z 500 hPa

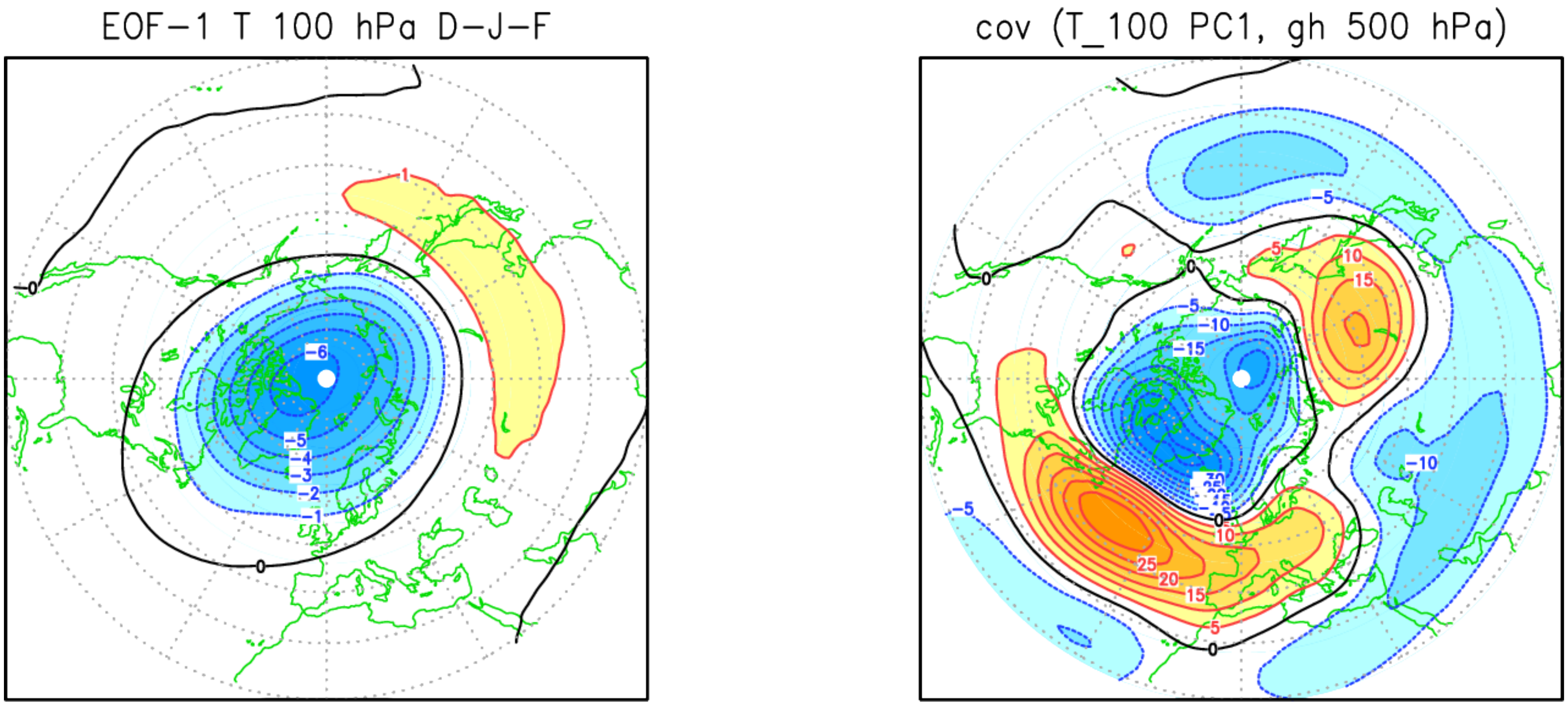

A role for the stratosphere (Fletcher, Kushner, Cassou 2010/2013/2015)

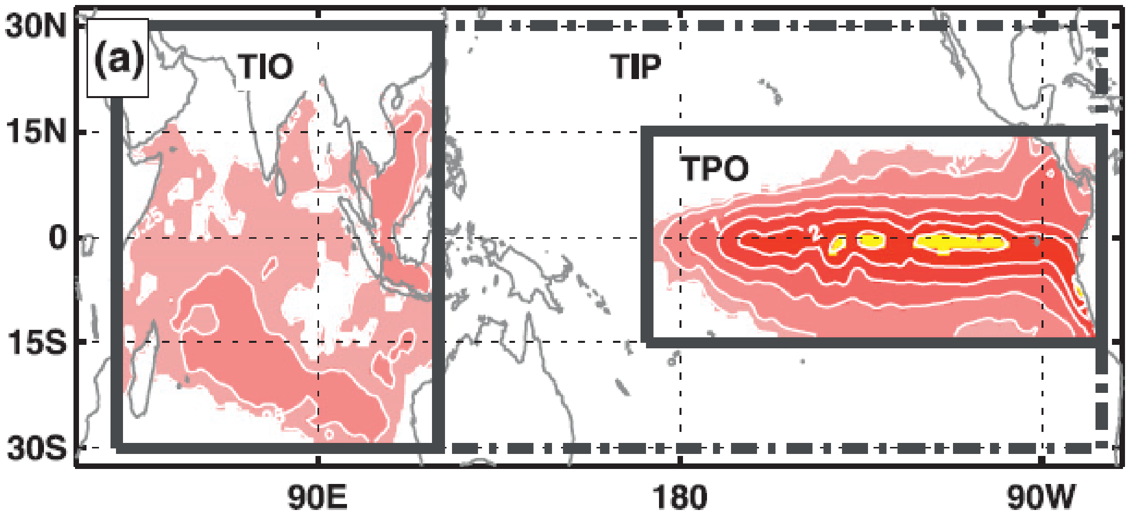

Fletcher & Kushner 2010

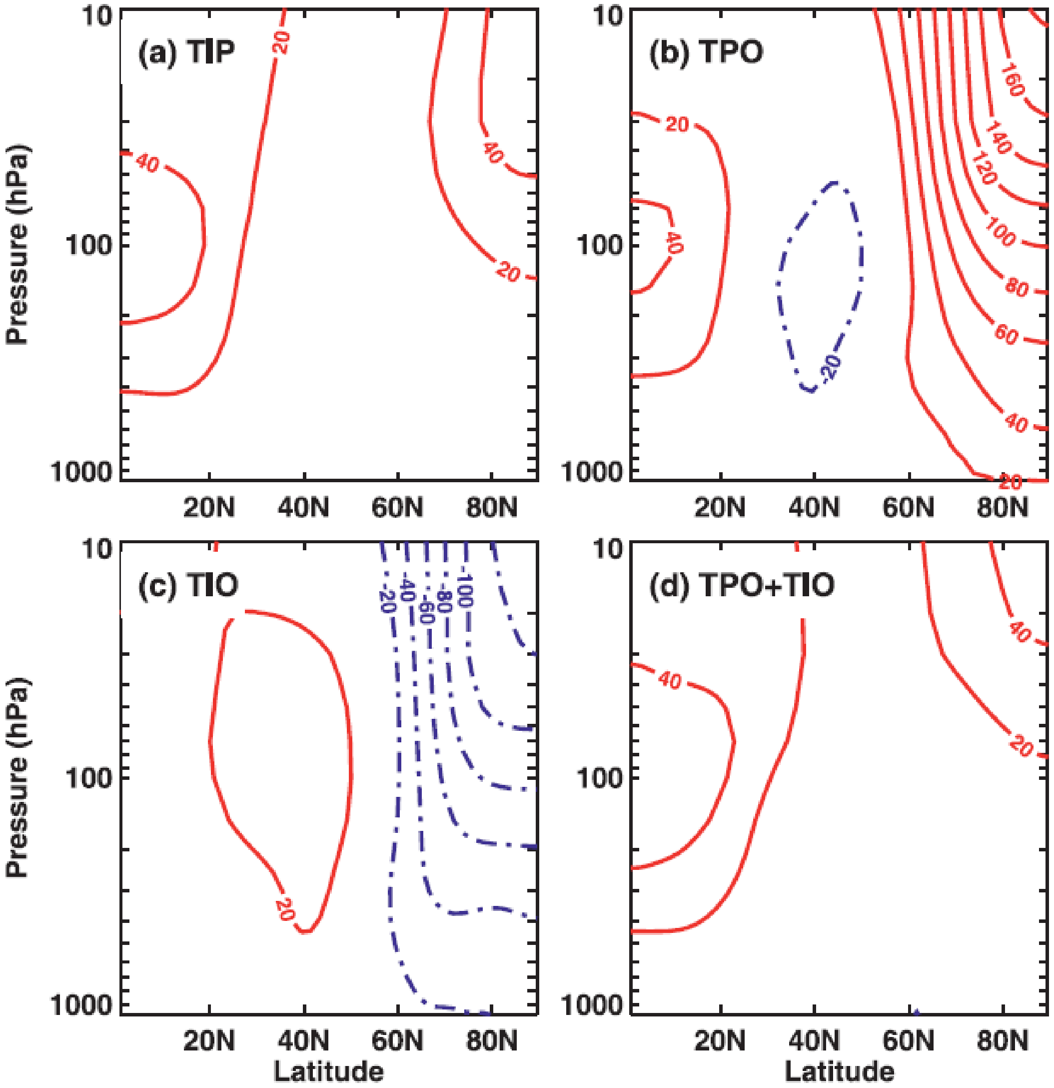

FIG. 5. The ensemble-mean JF zonal mean geopotential height response as a function of latitude and pressure in (a) TIP, (b) TPO, (c) TIO, and (d) the sum of the TPO and TIO responses. The contour interval is 20 m and negative contours are dashed.

Zonal mean heat transport [v*T*] in the lower stratosphere

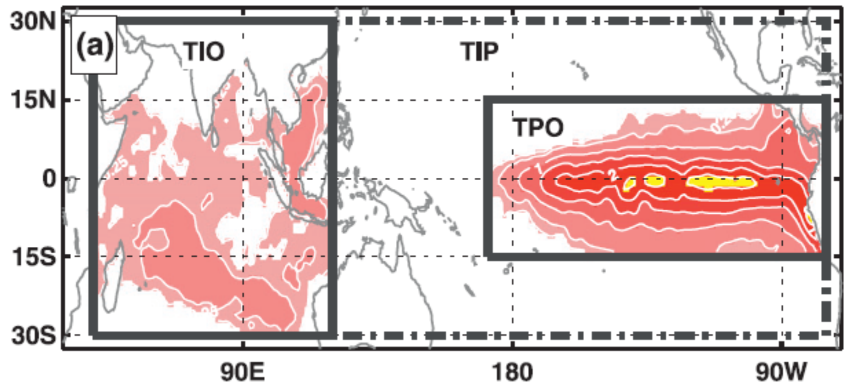

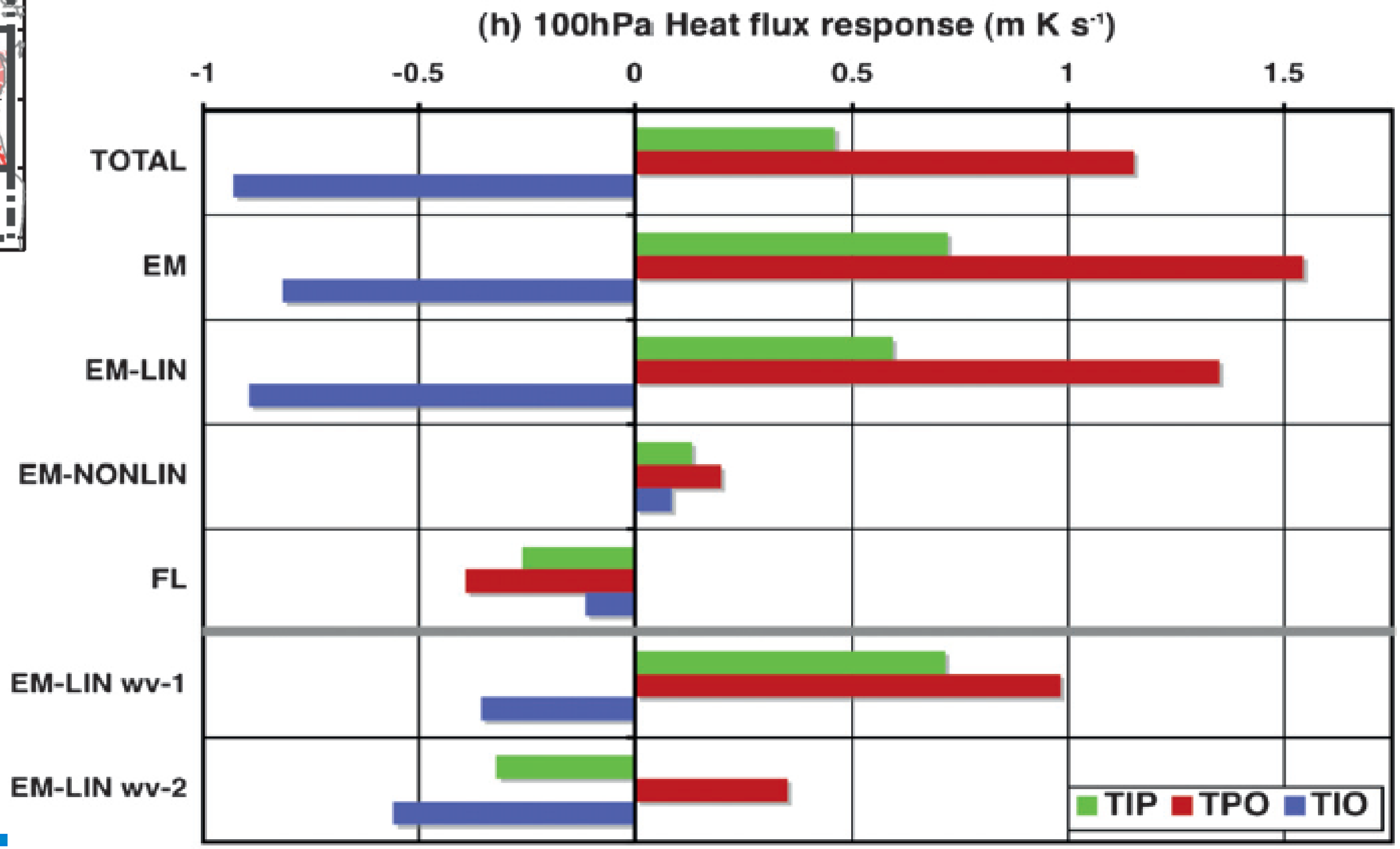

Summary

- Flow regimes in the North Atlantic and North Pacific sectors can be detected independently and explained by dynamical interactions on a regional scale.
- Teleconnections from tropical rainfall anomalies can create preferred combinations of Atlantic and Pacific regimes, and particularly a planetary wavenumber-2 regime with anomalies of the same sign on the northern side of both oceans (~ COWL pattern). This occurs when rainfall anomalies of the same sign and comparable amplitude exist in the W Indian Ocean and central Pacific.
- This teleconnections is important for both seasonal and decadal scales, and is also similar to the teleconnections from MJO phase 2-3. It is also related to anomalies in surface heat fluxes over the northern oceans.
- The Rossby waves originated by the Indian and Pacific ocean heating anomalies have opposite effects on the meridional heat flux convergence into the polar lower stratosphere/upper troposphere, creating opposite forcings on the polar vortex. In turn, this can affect the phase/intensity of the NAO response.